

INFORMATION TO USERS

This manuscript has been reproduced from the microfilm master. UMI films the text directly from the original or copy submitted. Thus, some thesis and dissertation copies are in typewriter face, while others may be from any type of computer printer.

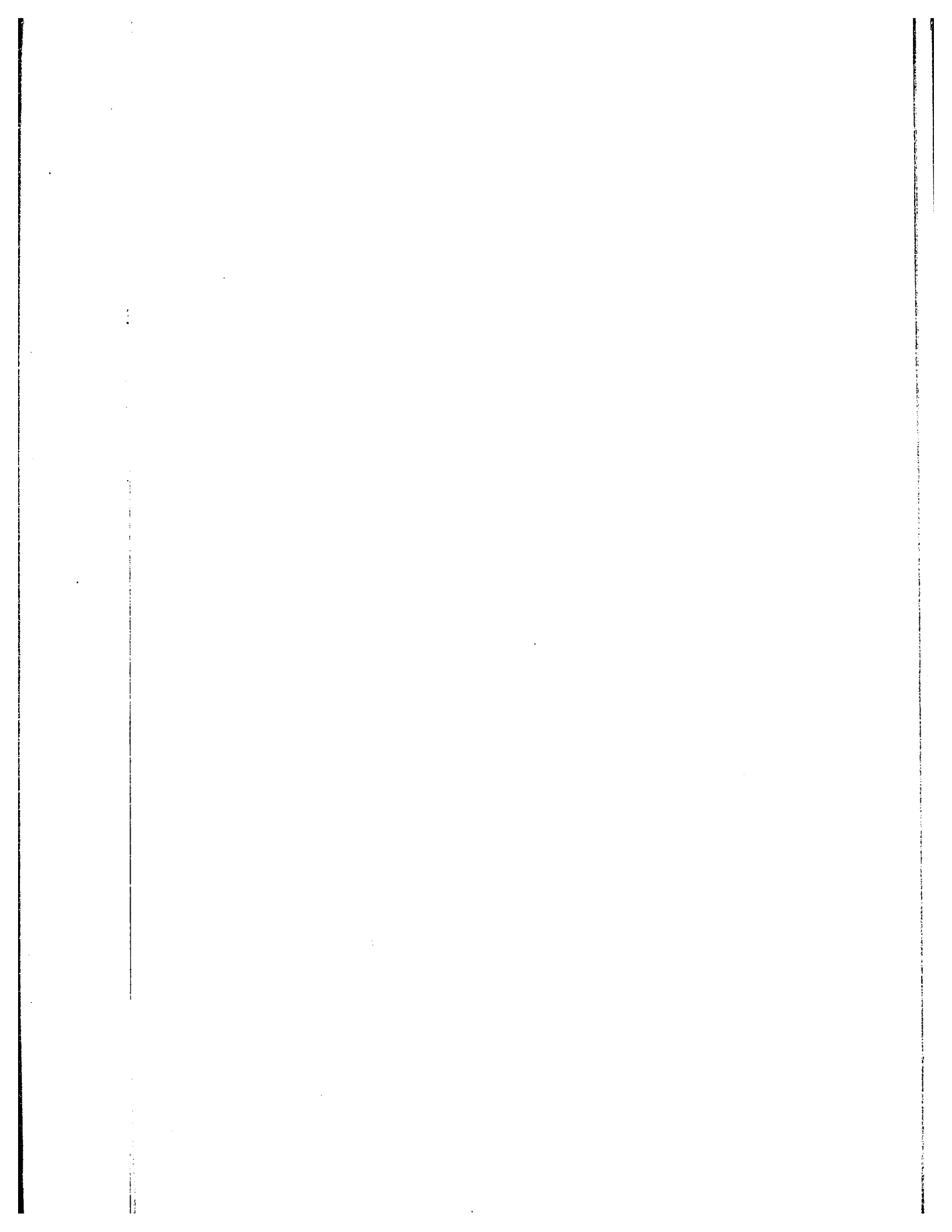
The quality of this reproduction is dependent upon the quality of the copy submitted. Broken or indistinct print, colored or poor quality illustrations and photographs, print bleedthrough, substandard margins, and improper alignment can adversely affect reproduction.

In the unlikely event that the author did not send UMI a complete manuscript and there are missing pages, these will be noted. Also, if unauthorized copyright material had to be removed, a note will indicate the deletion.

Oversize materials (e.g., maps, drawings, charts) are reproduced by sectioning the original, beginning at the upper left-hand corner and continuing from left to right in equal sections with small overlaps.

ProQuest Information and Learning
300 North Zeeb Road, Ann Arbor, MI 48106-1346 USA
800-521-0600

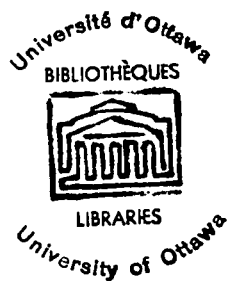
UMI[®]



THE APPLICATION OF HALL EFFECT
DEVICE FOR THE MEASUREMENT OF
LOW MAGNETIC FIELD

By

NAZIR A. CHAUDHRY



Submitted in partial fulfilment
of the requirements for the degree of
Master of Science
in Electrical Engineering

Department of Electrical Engineering
Faculty of Pure and Applied Science
University of Ottawa
Ottawa, Canada.
March, 1965.

UMI Number: EC52218

INFORMATION TO USERS

The quality of this reproduction is dependent upon the quality of the copy submitted. Broken or indistinct print, colored or poor quality illustrations and photographs, print bleed-through, substandard margins, and improper alignment can adversely affect reproduction.

In the unlikely event that the author did not send a complete manuscript and there are missing pages, these will be noted. Also, if unauthorized copyright material had to be removed, a note will indicate the deletion.

UMI[®]

UMI Microform EC52218
Copyright 2007 by ProQuest LLC
All rights reserved. This microform edition is protected against
unauthorized copying under Title 17, United States Code.

ProQuest LLC
789 East Eisenhower Parkway
P.O. Box 1346
Ann Arbor, MI 48106-1346

Approved for the
Department of Electrical Engineering

Supervisor

Chairman of the ~~Examining~~ Committee

Chairman of the Department

ABSTRACT

An indium antimonide Hall element is prepared, operated at liquid nitrogen temperature in combination with 5 inch long mumetal concentrator. The polycrystalline indium antimonide Hall probe provides an overall sensitivity of 12500 Volts/ampere-kilo gauss. The device is capable of measuring down to 2×10^5 gauss peak in the frequency range dc to 25 c/s. The factors which restrict the lowest limit of magnetic field detection are discussed and methods are suggested to further improve the sensitivity of the device.

ACKNOWLEDGEMENTS

The author expresses his profound gratitude to Professor G.S.Glinski, who suggested and patiently supervised this project.

The author also thanks Mr. J.Basinski of Northern Electric Company and Mr. A.Beck of National Research Council, Ottawa for useful suggestions as regards the preparation of the Hall element.

The author would like also to acknowledge the financial assistance for this project from the Colombo Plan of Canada and the Atomic Energy Commission of Pakistan.

TABLE OF CONTENTS

	<u>Page</u>
ABSTRACT	i
ACKNOWLEDGEMENT	ii
Introduction	1
CHAPTER I. Methods of Measuring Low Magnetic Fields :	3
1.1 Saturable-Core Magnetometer	3
1.2 Rotating Coils	6
1.3 Nuclear Magnetic Resonance	7
1.4 Ballistic Galvanometer and Fluxmeter	8
1.5 Electronic Integrator	8
1.6 Optically Pumped Rubidium Vapor Magnetometer	13
1.7 Hall effect	14
CHAPTER II. Hall Element	16
2.1 Theory of Hall Effect	16
2.2 Element Parameters	18
2.3 Limiting Factors in the Measurement of Low Level field	21
I. Misalignment Voltage	22
II. Inductive Null Voltage	24
III. Sensitivity	25
IV. Thermomagnetic Effects	29
V. Magnetoresistance	31
VI. Temperature Effect	31
VII. Noise	33

2.4 Choice of Material	36
CHAPTER III. Magnetic Flux Concentrator	42
3.1 Introduction	42
3.2 Self Demagnetization	43
3.3 Leakage Flux	47
CHAPTER IV. Experimental Work	49
4.1 Hall Element	49
4.2 Low Noise Amplifier	50
4.3 Production of Magnetic Field	50
4.4 Magnetic Flux Concentrator	52
4.5 Description of the Apparatus	53
4.6 Operation	57
4.7 Magnetic Gain of the Concentrator	58
4.8 Temperature Effects	58
4.9 Noise	59
4.10 Preparation of Hall Element	62
4.11 Results	65
Conclusion	71
References	74

INTRODUCTION

The measurement of low level magnetic field has not always been an easy task. Until recently, the convenient methods of measuring low magnetic field have been saturable core magnetometer, electronic integrator, nuclear magnetic resonance and optically pumped vapor magnetometer. These methods, although useful in certain respects, do not cover the following features as a whole: (I) absolute measurement. (II) Measurement of time varying magnetic fields and (III) Static magnetic fields. These devices are quite bulky and are not portable. This creates the need for having a practical, reasonably economical, compact and accurate low level magnetic field sensing device for the study of low frequency magnetic environments.

Very little work has been done towards the detection of low level magnetic field employing Hall effect device. The Hall effect was first discovered in 1879 in metal strips, but due to very low Hall voltage in metals, this effect could not be used for practical purposes. With the development in semiconductor materials in recent years, the properties of indium arsenide, indium antimonide, germanium and silicon etc. are such as to make them suitable for Hall effect device.

It is the purpose of this work to measure the low level magnetic field employing Hall effect device. Indium Antimonide material is selected for this purpose and a Hall probe is prepared and operated at liquid nitrogen temperature. Hall probe, magnetic concentrator and a low noise amplifier are combined to form a sensitive low magnetic field sensing device.

CHAPTER 1

METHODS OF MEASURING LOW MAGNETIC FIELDS

The development of science and technology has given rise to the problem of detection and measurement of ultra low and very high magnetic fields. The advancement in magnetic measurement techniques has been stimulated by the need for measurements in new or more stringent conditions. Some of the incentives to such a considerable development in magnetic measurement techniques are, for instance, magnetic field studies in outer space, low intensity measurements for geophysical studies of earth's field, complex type high field magnetic measurements in large particle accelerators and ultra low level measurements of biological magnetic field. In all these cases we are faced with the problem of accurately measuring a magnetic field which often varies both in space and time.

The present review is mainly concerned with low magnetic field measuring devices. The following methods are widely used for this purpose.

1.1 SATURABLE-CORE MAGNETOMETER

The underlying principle of this measuring device depends upon the fact that if a straight core, consisting of a wire of high permeability alloy, such as permalloy or Mumetal, is excited by a sinusoidal field of sufficient amplitude to drive

it well into saturation, the resulting voltage wave form induced in the search coil around the core is distorted in the presence of external d c field, and contains even and odd harmonics of the exciting frequency. The amplitudes of the harmonics are functions of the applied field along the core. Since the amplitude of the second harmonic is roughly proportional to the applied field, it is separated and measured. Its value gives the unknown magnetic field along the core.(1)

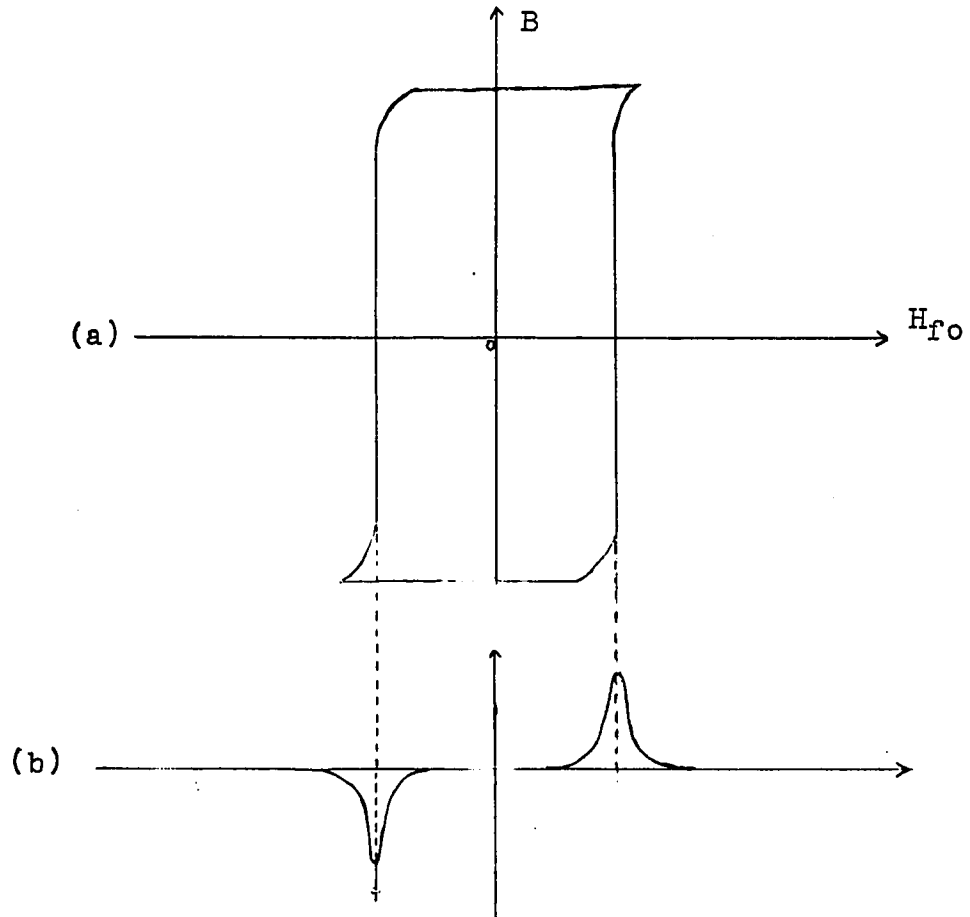


Fig. 1.1 (a) B-H loop of the core in the absence of external dc field.
(b) Voltage waveform induced in the search coil.

The principle of operation of the device is *ill*ustrated in Fig. 1.1. When the primary coil of the device is driven by an exciting field H_{f_0} of frequency f_0 and there is no steady field component along the core, the hysteresis loop is as shown in Fig. 1.1a. The whole pattern is symmetrical with respect to zero field position. Fig. 1.1b shows the corresponding voltage in the search coil and contains only fundamental and odd harmonics of f_0 . If a biasing field is produced by passing a dc current in the primary, the B-H loop becomes asymmetrical. The induced voltage waveform will be distorted and will contain even and odd harmonics of the exciting frequency.

The magnetic field along the axis of the core can be measured in either of the following ways:

1. The output of the search coil is fed to an amplifier which is tuned to the second harmonic of the exciting frequency. The amplified output is calibrated against the field of a Helmholtz Coil.
2. The core is biased with dc field in the proper direction, so that the amplified output is reduced to zero. The bias current is calibrated against a standard magnetic field source.

The principle of saturable core is utilized by McCurley and Blake (2) in the development of their magnetometer. The second harmonic of the exciting frequency of 5 kc is amplified by the tuned amplifier.

60 c/s ac pick up field appears as amplitude modulation of the output of the tuned amplifier. The device measures the dc magnetic field down to 10^4 gauss.

Recently, Vickers magnetometer PM 1 (3) claimed a lower limit of 10^5 gauss in the frequency range of .04—.2c/s.

1.2 ROTATING COILS

A sinusoidal Voltage V is induced in a search coil, which is rotated at constant angular velocity w, about an axis perpendicular to the magnetic field and is given by

$$V = N S W B_n 10^8 \text{ volts}$$

where N = Number of turns in the coil.

S = Mean area of one turn. (cm^2)

B_n = Magnetic flux density perpendicular to the axis of rotation. (Gauss)

Signal from the search coil is picked up from slip rings, amplified, rectified and measured. To obtain greater accuracy, two coils are used, one in the field to be measured and a second coil on the same shaft in the variable known field of a Helmholtz Coil. The search coil voltages are connected in opposition and an amplifier is used to detect the null.

The sliding contacts can be eliminated by using a coupling transformer whose primary winding is connected to the sensing coil and rotates with it, whereas the secondary is fixed as shown in Fig. 1.2 (4)

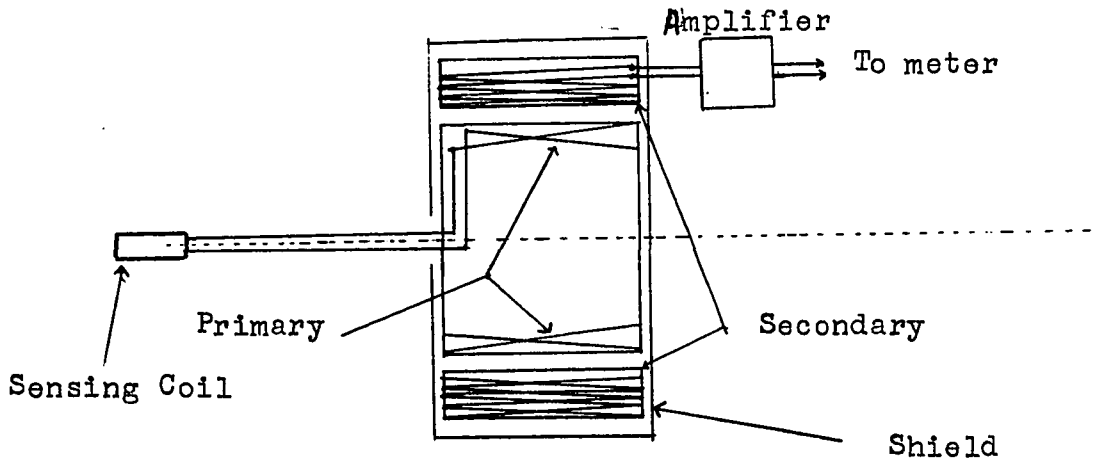


Fig. 1.2

Rotating Coil Magnetometer

The sensitivity of the instrument is limited by the variations in speed of the motor rotation, noise due to elastic mechanical vibrations, fluctuations due to the displacement of the coil and pick up interference.

Changes in the ambient field of the order of 10^{-3} Gauss can be detected with a rotating coil magnetometer. (5)

1.3 NUCLEAR MAGNETIC RESONANCE

The free precession of a nucleus in an external magnetic field B has an angular frequency ω given by (6)

$$\omega = gB \dots \dots \dots 1.2$$

Where g is the nuclear gyromagnetic ratio

Absolute field values are obtained by measuring the Larmor frequency

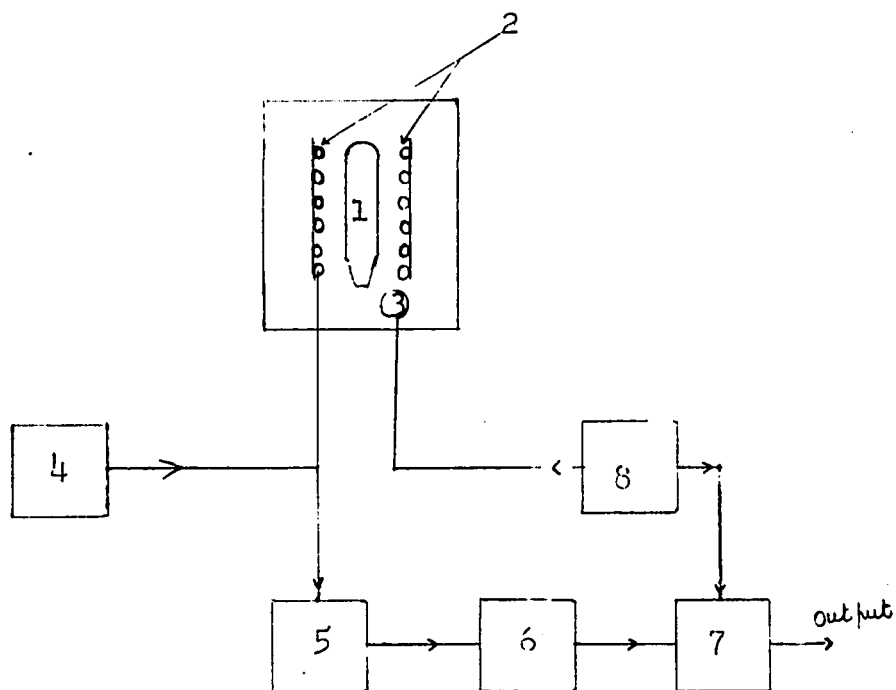
$$f = \frac{\omega}{2\pi} = \frac{g}{2\pi} B \dots \dots \dots 1.3$$

The magnetic resonance apparatus consists of two parts: one for producing the oscillating magnetic field, and the other for

detecting the magnetic resonance which can be done either by bridge method or the induction method. The oscillating magnetic field is usually produced in a small emitting coil containing the resonating sample, oriented so that its axis is perpendicular to the magnetic field B. When the oscillating field is in resonance with the Larmor frequency, nuclear resonance takes place. In the bridge method (Fig. 1.3) this results in unbalancing the bridge. The signal from the bridge network is amplified by a narrow bandwidth audio amplifier and fed into a mixer. In the mixer the signal beats against the sweep voltage producing a dc voltage proportional to the amplitude of the signal. The frequency of the signal generator corresponding to the maximum output is measured and substituted in eq. 1.3 to obtain the magnetic intensity B.

In the Induction method, another pickup coil having the sample, is oriented at right angle to the emitting coil, so as to reduce the inductive coupling as much as possible. For frequencies near the magnetic resonance, an oscillating voltage is set up in the pick up coil, which is amplified and detected. Thus knowing the frequency at which magnetic resonance takes place, the magnetic field is calculated from Eq. 1.3. The accuracy of the measurement depends upon two factors, the nuclear constant and the frequency of precession.(7) For proton, g has been measured with an accuracy of $\pm 2 \times 10^{-5}$ per secper gauss. Accuracy is limited only by the accuracy of measurement of frequency.

The value of earth's horizontal component is measured with



1. Sample in a glass tube.
2. Emitting Coil.
3. Sweep Coil.
4. Signal Generator.
5. Bridge Network.
6. Narrow Band Audio Amplifier.
7. Mixer.
8. Low Audio Sweep Generator.

Fig. 1.3

Nuclear Resonance Magnetometer

an error of 0.3×10^5 gauss (8).

1.4 BALLISTIC GALVANOMETER AND FLUXMETER

Ballistic galvanometer and fluxmeter directly measure the variation of the magnetic flux linking a search coil. A voltage is induced in the search coil by the changing magnetic flux. An integrator is used, so that the flux density rather than its time derivative is obtained.

A fluxmeter serves the purpose of a mechanical voltage integrator, the deviation of the fluxmeter pointer gives the value $\Delta\phi = \int \left(\frac{d\phi}{dt}\right) dt$ which is integrated value of the voltage $\frac{d\phi}{dt}$ applied at its terminals. Ballistic galvanometer due to its long time period, enables us to measure fields of duration less than 1 sec.

When comparing the flux values of two separate coils, one in the reference field, the balance method makes it possible to attain high accuracy with either the fluxmeter or the ballistic galvanometer. The galvanometer or fluxmeter is used as a null reading instrument and any small disbalance is detected.

The sensitivity is usually limited to about 10^1 gauss but it can be pushed to about 10^3 gauss provided precautions are taken against thermal and contact e.m.f.'s. (9) (10) (11).

1.5 ELECTRONIC INTEGRATER

If the field is changing in time and its value at any instant is required, the induced voltage must be integrated. The voltage is induced in a flat coil with n turns, when placed in an alternating magnetic field. An integrating R-L or R-C network can be employed to integrate the output of the coil. An induced e.m.f. in case of sinusoidal magnetic field strength B

is given by

$$E = n A \omega B_m \cos \omega t \cos \phi \quad 1.4$$

where B_m = amplitude of the magnetic field strength

A = area of the windings

ω = angular Velocity of the magnetic field

ϕ = angle between the magnetic field strength B and the normal to the plane of the coil windings.

$$E = n A \omega B_m \cos \omega t \quad \text{for } \phi = 0^\circ \quad 1.5$$

From Eq. 1.5 it is clear that E is proportional not only to B_m but also to frequency $\frac{\omega}{2\pi}$.

The integrating network eliminates the effect of frequency.

The voltage V_1 at the output of the integrating network R-C

Fig. 1.4 is given by

$$V_1 = \frac{n A B_m \sin \omega t}{\left(R + r + \frac{1}{j\omega C} \right) C} \quad 1.6$$

Where r is the resistance of the coil.

In the case of perfect integrator we have

$$R+r \gg \frac{1}{\omega C}$$

$$\text{then let } V_1 = V_2 = \frac{n A B_m \sin \omega t}{(R+r) C} \quad 1.7$$

$$= K B_m \sin \omega t \quad 1.7a$$

$$\text{Where } K = \frac{n A}{(R+r) C}$$

The frequency error δ is given by (12)

$$\delta = \left| \frac{V_2 - V_1}{V_2} \right|$$

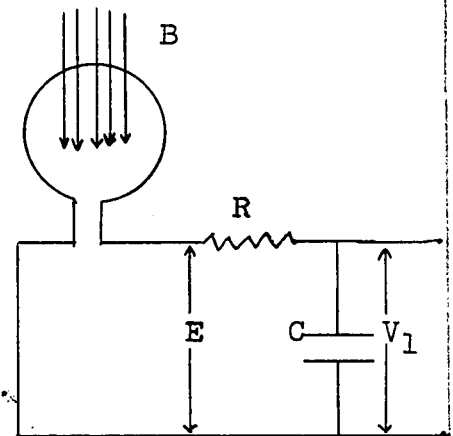


Fig. 1.4

RC Integrating Network

For R-C network $\delta_C = \frac{1}{2} \frac{1}{\omega(R+r)C} \times 100\% \dots\dots 1.8$

In the case of R-L network $\delta_L = \frac{1}{2} \frac{(R+r)}{\omega L} \times 100\% \dots 1.9$

The frequency error δ decreases with an increasing frequency of magnetic field. The error can be decreased by using an integrator having large time constant. For instance, Miller integrator (13), which is essentially a d.c amplifier with a high gain G. Fig 1.5. It integrates the input voltage during a time which is G time longer than in simple RC circuit.

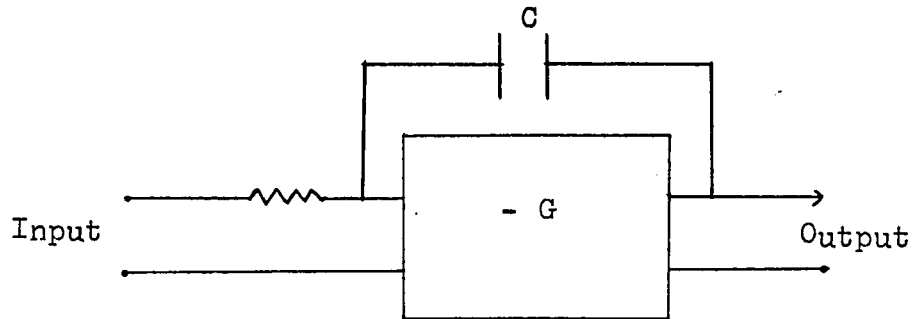


Fig. 1.5
Miller Integrator

For higher sensitivity, search coil can be wound on a high permeability material, which can magnify the unknown magnetic field few hundred times. When very accurate measurements are required, two coils of identical characteristics are used side by side in series opposition. (14)

Any stray alternating magnetic field whose origin lies quite far away from the coils, will induce equal and opposite voltage in each coil, thus making the net output zero. Output

will only be detected when an unknown field is applied to one coil.

The induced e.m.f. and the current produced by it in the coil increase with frequency. This current produces magnetic field which according to Lenz law operates in the opposite direction to the unknown field being measured. Since the resulting voltage in the coil depends not only on the measured field, but also on the opposing field, the latter has to be taken into account.

The integrator method provides a good accuracy for measuring time varying magnetic fields and a sensitivity of 10^{-6} Gauss peak value has been claimed. (14) The measurement however yields the mean value over the coil area.

1.6 OPTICALLY PUMPED RUBIDIUM VAPOUR MAGNETOMETER

Optical pumping consists of raising atoms from a low energy state to a higher energy state. Rubidium Vapour is used as a pumping material. In the absence of external influence, the electrons of the rubidium atoms will be in the unexcited or ground state. To pump electrons to the P-state or excited state, it is necessary to expend energy. Electrons can be excited to the P-state by bombardment with electrons or ion beam or by irradiation with light of the correct wave length.

In practice, the rubidium vapour in a sealed gas cell is irradiated with light from a rubidium spectral lamp. When the rubidium atoms are placed in a magnetic field, the s-state energy level further splits into fine levels called the m level. Transitions between m level are magnetic field dependent and therefore can be used in a magnetometer system. (15)

With this process, the range of measurement is extended down to 1×10^{-5} gauss. (16)

1.7 HALL EFFECT

This effect was discovered in 1879 by Edward H. Hall. He observed that a voltage appears between the edges of a metal strip, when current carrying metal strip is placed in a magnetic field. The voltage that appears perpendicularly to the direction of the flow of the current is called "Hall Voltage" and is maximum when the magnetic field applied is perpendicular to the current.

This effect was relatively weak in gold and iron but one thousand times stronger in bismuth and fifty thousand times in tellurium. (17)

Due to developments in semiconductor materials, such as Germanium, Silicon, Indium Antimonide, Indium Arsenide, Gallium Arsenide, Gallium Antimonide and Indium Arsenide Phosphide, this effect acquired practical importance. Magnetic field strength can be measured by knowing the Hall Voltage which appears at the output terminals of the Hall generator and the control current flowing through it.

The open circuit Hall Voltage is given by the equation

$$V_H = R_H \frac{I}{t} B \times 10^{-8} \text{ Volts} \dots\dots\dots 1.10$$

where R_H = Hall coefficient in $\text{cm}^3 / \text{coulomb}$

B = Magnetic field strength in Gauss

I = Control Current in amperes

t = Thickness of the Hall element in cm.

Since $\frac{R_H}{t}$ is a constant of a particular Hall element used at a

certain temperature, then V_H can be calibrated in terms of magnetic field strength B for a particular control current I .

This method is capable of measuring dc as well as ac magnetic fields up to few thousands of magacycles. (18)

Magnetic field down to 10^{-5} Gauss can be measured using indium Antimonide material for Hall element in combination with magnetic concentrator. (19)

The limit to the detection of the lowest magnetic field is set by the thermal drift due to temperature instability and the noise voltage originating from the Hall element in the absence of the magnetic field being measured. The factors which affect the performance of the Hall element are discussed in the next chapter.

Hall effect device provides a simple method for the measurement of magnetic field. It permits direct determination of a magnetic field without measuring a time rate of change and integrating. Due to its small size, high sensitivity and ability to measure steady as well as varying fields, it is preferred over other conventional methods.

CHAPTER II
HALL ELEMENT

2.1 THEORY OF HALL EFFECT

Fig. 2.1 is a typical Hall element of length l , breadth b and thickness t , having perfectly conducting electrodes of finite size.

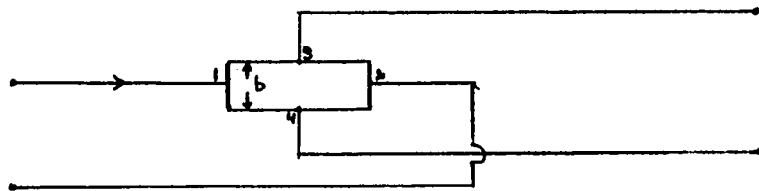


Fig. 2.1

Control current density and magnetic field are assumed constant and uniform. When voltage is applied to the control terminals 1 and 2, the current consists of charged particles drifting under the influence of electric field. With magnetic field absent, the current flows longitudinally in the element. When a magnetic field B is applied, the current carriers experience a Lorentz force $e\vec{v} \times \vec{B}$ in a direction mutually perpendicular to both \vec{v} and \vec{B} , where e and v are electronic charge and drift Velocity of carriers respectively. The charge continues to build up on the edges of the element, until the electric field due to non-uniform charge distribution exerts a force equal but opposite to the deflecting Lorentz force.

$$\frac{V_H}{b} e = e\vec{v} \times \vec{B} \dots\dots\dots 2.1$$

$$V_H = bvB \sin\theta \dots\dots\dots 2.2$$

where V_H = Hall voltage.

v = drift velocity of carriers in cm/sec.

b = breadth of the element in cm.

B = flux density in gauss.

θ = angle between current direction and flux density.

Current density J can be introduced in eq. 2.2

$J = nev$ where n is carrier concentration per unit volume

Eq. 2.2 becomes

$$V_H = \frac{bJ}{ne} B \sin \theta$$

$$= \frac{1}{net} IB \sin \theta$$

since $I = Jbt$

$$= \frac{R_H}{t} IB \sin \theta \times 10^{-8} \text{ Volts} \dots\dots\dots 2.3$$

where 10^{-8} is introduced as the conversion factor for the system of units selected.

and $R_H = \frac{1}{ne}$ $\text{cm}^3/\text{coulomb}$ is called the Hall Coefficient.

$$\dots\dots\dots 2.3a$$

For transverse magnetic field, $\theta = 90$ degrees.

$$V_H = \frac{R_H}{t} I B 10^{-8} \text{ Volts} \dots\dots\dots 2.4$$

$$= SIB 10^{-3} \text{ Volts} \dots\dots\dots 2.4a$$

Where S is the sensitivity of the Hall element (volts/ampere-kilo gauss), I control current in amperes and B = magnetic flux density in ~~gauss~~-gauss.

The sensitivity is the proportionality factor for a particular Hall element. It determines the open circuit Hall voltage for one ampere control current and one kilo-gauss magnetic field.

2.2 ELEMENT PARAMETERS

Important parameters of the Hall generator are defined and discussed below:

1. Input Resistance
2. Output Resistance
3. Sensitivity
4. Misalignment Voltage
5. Inductive null Voltage
6. Temperature dependence

1. INPUT RESISTANCE: It is the resistance of the Hall element as measured between terminals 1 and 2 (Fig. 2.1) and is denoted by R_i . It determines the operating control current one may pass through the element at a particular heat dissipation of the element. This resistance is dependent on temperature of the element and is plotted against temperature for a particular Hall element (Beckman, model 335) (Fig. 2.2).

2. OUTPUT RESISTANCE: This is the resistance measured between terminals 3 and 4 (Fig. 2.1). This parameter, like the first one, is also temperature dependent.

3. SENSITIVITY: This term is defined by the equation 2.4a. The effect of control current can be included in the definition of sensitivity. Then the sensitivity will determine the Hall Voltage for a given magnetic field. Therefore, sensitivity can better be defined as the open circuit Hall Voltage for a magnetic field of one gauss at the operating control current. For low level measurement of magnetic field it is necessary to have a Hall element of high sensitivity, so that it may produce a

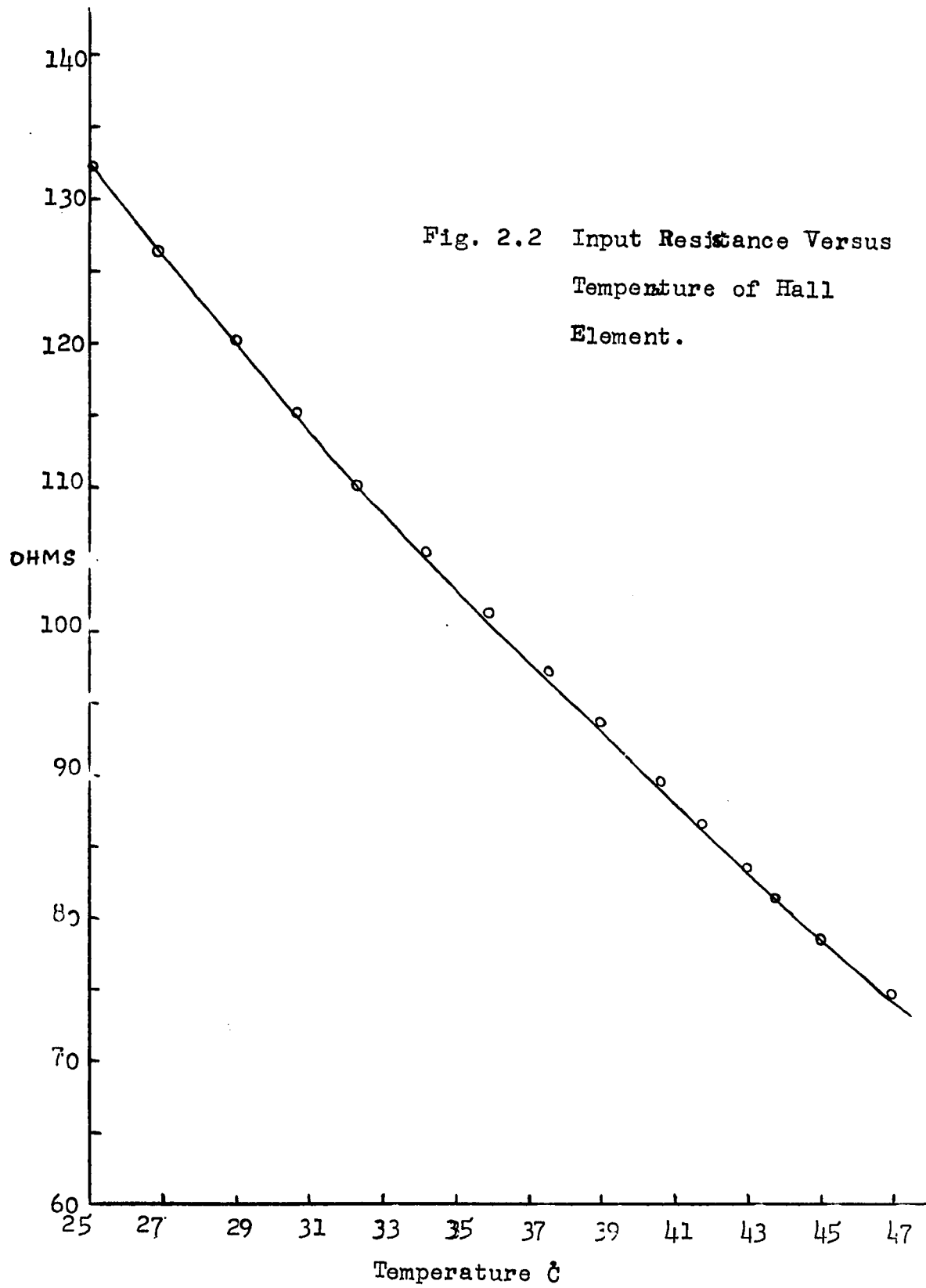


Fig. 2.2 Input Resistance Versus Temperature of Hall Element.

measurable Hall Voltage at the lowest field to be detected.

4. MISALIGNMENT VOLTAGE: Misalignment Voltage is also called "Zero field voltage" or "Resistive Null" and is the voltage appearing between the terminals 3 and 4 (Fig. 2.3) when a current flows in the element and the magnetic field is zero.

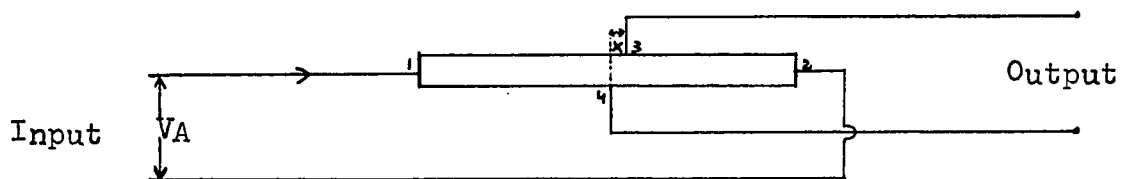


Fig. 2.3 Misalignment Voltage caused by non-symmetric placement of Hall output electrodes.

This voltage arises because the output contacts do not lie exactly on an equipotential across the width of the element. The two major components of this voltage are both dependent upon the control current. The first component is linear with the control I or the applied voltage V_A and is given by the relation:

$$V = \frac{x}{L} V_A \text{ where } x \text{ is shown in Fig. 2.3}$$

The second component is non-linear, depending upon square of the control current and is due to power dissipation effects. In the next section ("Limiting factors in the measurement of low level field"), the effect of misalignment will be discussed and methods described to reduce this effect.

5. INDUCTIVE NULL VOLTAGE: This voltage is caused by the pick up loop formed in the output circuit of a Hall element as shown in Fig. 2.4.

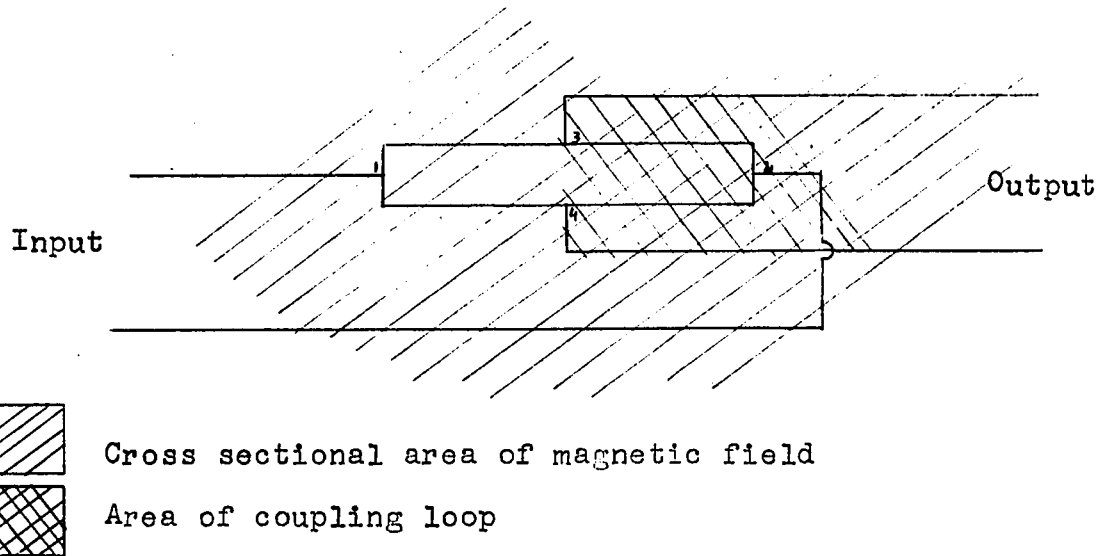


Fig. 2.4

It is proportional to the cross hatched area. It is present only when the magnetic field being measured is time varying and depends upon the time rate of change of the magnetic field. An undesired voltage is also induced in the output when ac current flows through the Hall element in the absence of the magnetic field. By careful adjustment of the orientation of the output leads, this method may be reduced. Methods to minimize this voltage are described in the next section.

6. TEMPERATURE DEPENDENCE: The Hall voltage decreases in a non-linear manner with increasing temperature. The changes in Hall voltage are due to the fact that input and output resistance and Hall coefficient are temperature dependent. These variations in the Hall output can be compensated by suitable associated circuitry described in the next section.

2.3 LIMITING FACTORS IN THE MEASUREMENT OF LOW LEVEL FIELD

The Hall voltage is influenced by many extraneous factors. The interference will not generally affect the large signal, however, low level signals may be completely lost in the noise.

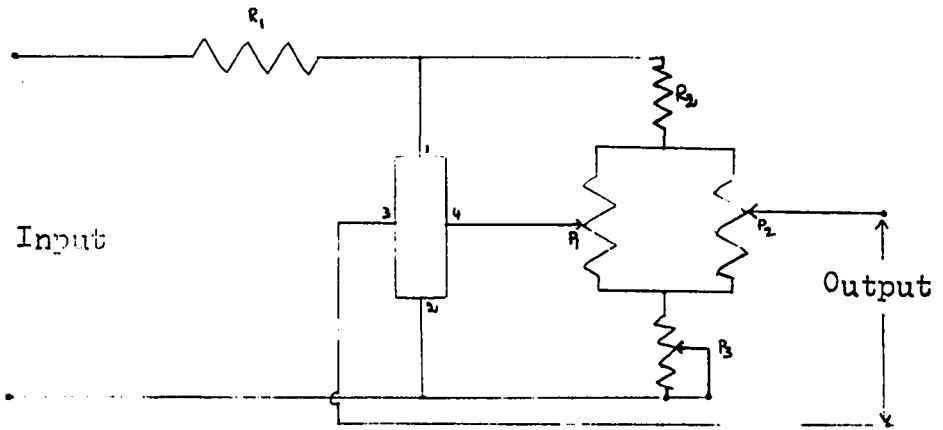
We will examine in details the practical possibility of using this device for the measurement of low magnetic fields. Limiting factors will be analysed and a practical approach to minimize their effects will be adopted.

In the following we shall systematically analyse the limiting factors involved:

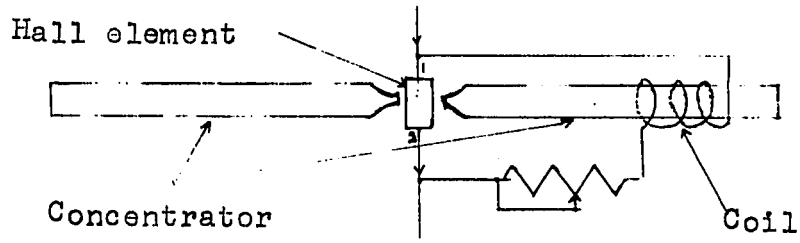
- (I) Misalignment voltage
- (II) Inductive null voltage
- (III) Sensitivity
- (IV) Thermo-magnetic effects
- (V) Magnetoresistance
- (VI) Temperature effect
- (VII) Noise

(I) MISALIGNMENT VOLTAGE: This voltage is dependent on the control current and the resistivity of the material. Variations in resistivity due to the variations from point to point in thickness and size of the Hall element may lead to fluctuations in this non-linear voltage. It is desirable to reduce this voltage to a negligible value as compared with the required Hall output. This, in turn, will depend upon the manufacturing techniques and the external circuitry employed to reduced this voltage. The misalignment voltage can be compensated in a number of ways:

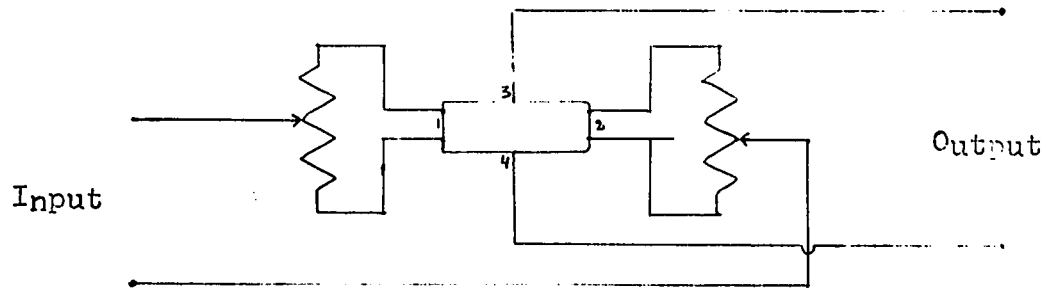
1. Modified form of the circuit suggested by Kuhrt (20) is shown in Fig. 2.5a. By adjustment of the potentiometers P_1 , P_2 , and P_3 , current is fed into the Hall output terminal to alter the equipotentials and resistive null is reduced to zero. This adjustment will work for one particular value of the control current.



(a)



(b)



(c)

Fig. 2.5
Compensation of misalignment voltage

2. Misalignment voltage can be reduced by supplying a small magnetic field from a solenoid. This is illustrated in the Fig. 2.5b. Few turns on concentrator rod, form a solenoid which is connected in series through a variable resistor with the control current. The adjustment of the compensating system is carried as follows:

The winding is moved axially along the rod, until the magnetic field, it generates in the air gap, results in a Hall voltage equal but in opposition to the zero field Hall voltage. Fine adjustment can be made by adjusting the variable resistor. This adjustment also holds for one particular value of the current. This method does not change the output impedance of the Hall element.

3. Roth and Straub (21) used an ingenious method to compensate the voltage. The arrangement is shown in Fig. 2.5c. Hall contacts can be located on a equipotential surface by modifying the current distribution. They reduced the misalignment voltage to $.2\mu\text{v}$ over the entire current range from 0 to 100 mA.

(II) INDUCTIVE NULL VOLTAGE: Spurious voltages are induced in the output, due to the ac control current and the ac magnetic field and limit the frequency response of the Hall element as well as decrease the signal to noise ratio.

Methods are described to minimize this effect:

1. One output terminal is joined to the sliding contact of the potentiometer P which is connected across a coil wound on the one side of the concentrator. (Fig. 2.6a). By adjusting the arm of the potentiometer, the induced voltage can be reduced considerably.
2. From one Hall output terminal, the leads are brought out in a symmetrical double loop through a potentiometer. (22). The Hall output connection is then taken as a variable tap on the potentiometer, which may be adjusted to a zero pick up position. A similar device is used in the input circuit. (Fig. 2.6b).

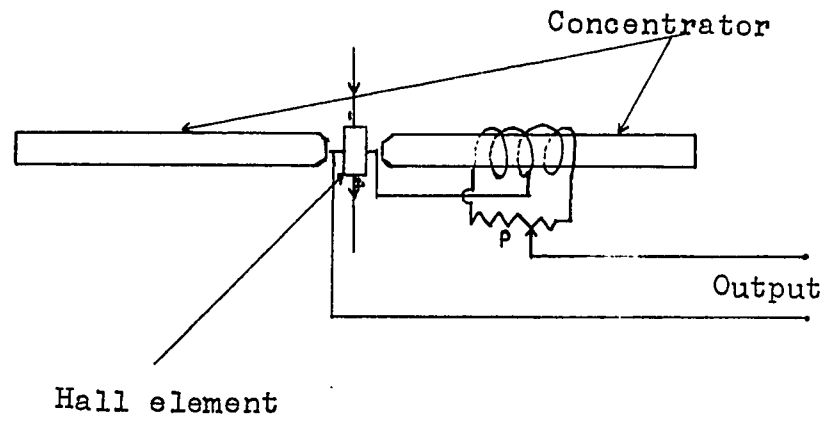
The induced voltage may also be cancelled if a voltage source were to supply an equal and opposite voltage.

(III) SENSITIVITY: The main criterion of selecting a Hall element for measurement of low field, is that it must have high sensitivity. The sensitivity of Hall element can be increased by suitable changes in thickness, carrier density and length to width ratio. Further increase is obtained by cooling the material and increasing the magnetic flux density. These factors are discussed below:

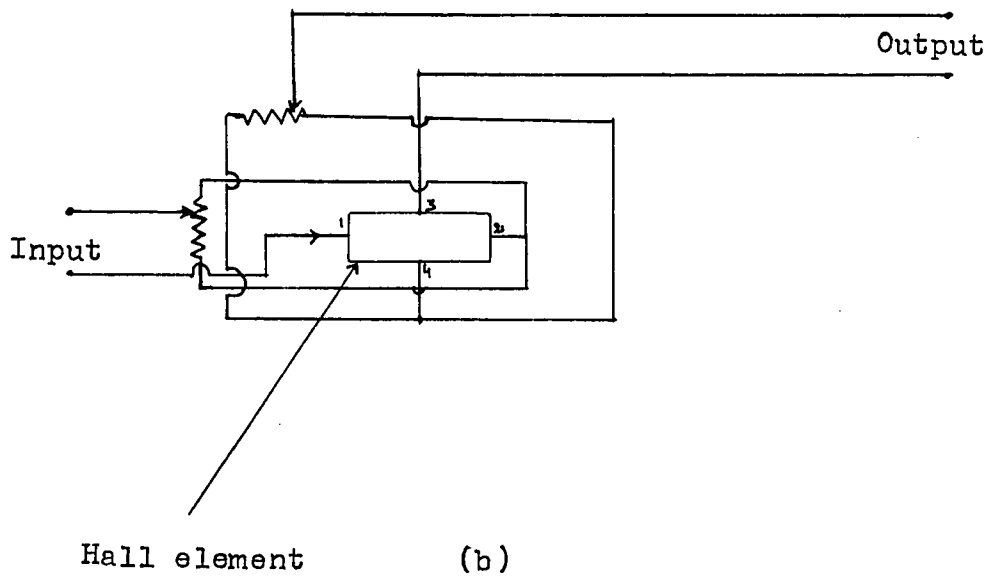
1. EFFECT OF THICKNESS:

From eq. 2.4, we have $V_H \propto \frac{1}{t}$

This relation states that Hall voltage and hence the sensitivity increases with the decrease in thickness of the Hall element. The decrease in the thickness is limited by the fabrication problems,



(a)



(b)

Fig. 2.6

Induced Voltage Compensation

difficulty in handling the element and the heat dissipation of the element. Some commercially available elements have thickness as low as .002 inch. The reduction in thickness does not produce proportional gain due to power dissipation as shown in the section "on choice of material." (Eq. 2.12).

2. CARRIER DENSITY

From Eq. 2.3a, we have $R_H = \frac{1}{ne}$

where R_H = Hall coefficient

n = carrier concentration

e = charge of the carrier

The Hall coefficient and hence the sensitivity can be increased by decreasing the carrier density. The carrier density is related to the resistivity ρ of the material by the relation:

$$\rho = \frac{1}{ne\mu}$$

where μ = mobility of the carrier

The reduction in carrier density will result in the increase of resistivity of the material. Then power dissipation of the device will become a problem. In such case, the device should be operated in some coolant which immediately removes the heat dissipated.

3. LENGTH TO WIDTH RATIO

$$V_H = \frac{R_H}{t} \cdot IB \cdot 10^{-8} \text{ volts} \quad \dots\dots\dots 2.4$$

Eq. 2.4 holds only for an infinitely long Hall element,

ie $\frac{l}{b} \rightarrow \infty$. For finite dimensions, the Hall voltage

is decreased in proportion to the function $F(\frac{l}{b})$. (23). Values of $F(\frac{l}{b})$ have been computed (24) for the Hall voltage and are plotted in Fig. 2.7.

TABLE 2.1

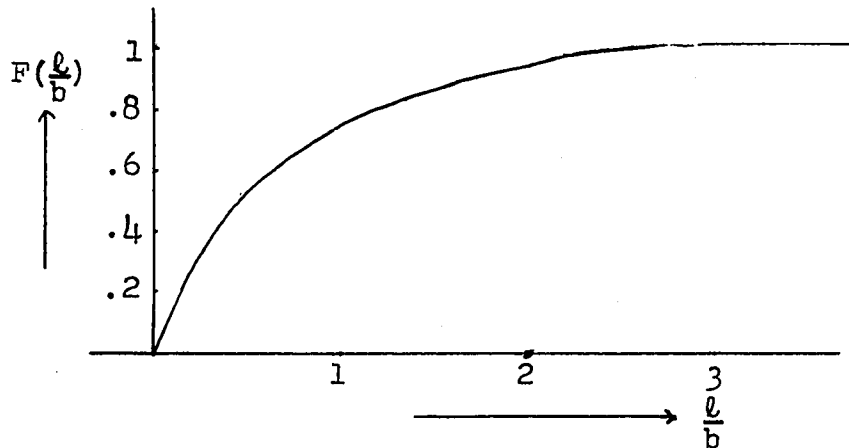
$\frac{l}{b}$	$F(\frac{l}{b})$
3	.98
2	.92
1.5	.88
1	.72
.5	.50
.25	.28

The function F is zero when l is zero but attains a value unity when the ratio $\frac{l}{b}$ is about 3. For larger values of this ratio, F remains unity. Introducing this function into equation 2.4, we have;

$$V_H = F(\frac{l}{b}) \frac{R_H}{t} I B 10^8 \text{ volts} \dots\dots\dots 2.5$$

Fig. 2.7

Variation of F
with $\frac{\text{length}}{\text{breadth}}$



The sensitivity of the Hall element can be increased by varying the dimensions of the element, keeping the thickness constant. Since maximum control current is directly related to the element width, the sensitivity is increased by increasing the width. The length

of the Hall element becomes important only when $\frac{l}{b}$ is < 3 . (Fig. 2.7.) Thus at a particular ratio of length to breadth, the sensitivity is increased with an increase in the width.

4. MAGNETIC FLUX DENSITY: The increase in this variable is made possible by the use of a magnetic flux concentrator which is discussed in the next chapter.

(IV) THERMO-MAGNETIC EFFECTS: The thermo-magnetic effects, such as, the Ettingshausen effect, the Nerst effect and the Righi-Leduc effect give rise to undesired voltages in the Hall output. (25) The thermoelectric effects, Peltier effect and Seebeck effect, produce transverse temperature difference and potential difference respectively in the Hall element. These effects are discussed below:

ETTINGSHAUSEN EFFECT Consider a specimen in the form of a rectangular plate of length l , breadth b and thickness t .

The Ettingshausen effect is the production of a temperature gradient between 3 and 4 (Fig. 2.8) when a current flows in the x-direction with a magnetic field in the Z-direction

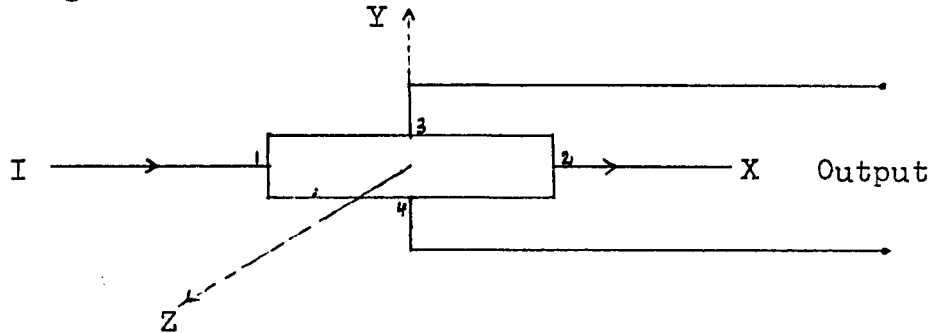


Fig. 2.8

The temperature gradient is found to be proportional to the product of the current density and the magnetic field.

$$\frac{T_1 - T_2}{b} = STB \dots\dots\dots 2.6$$

where T_1 and T_2 are the temperatures of junctions 3 and 4.

S = Etingshausen Coefficient

Eq. 2.6 can be written as

$$\Delta T = S \frac{I}{b} B \quad \dots \dots \dots 2.7$$

where I = Control current in the plate.

A thermo-electric potential difference will exist across the Hall output terminals due to the Etingshausen temperature gradient given by Eq. 2.7.

NERST EFFECT: A potential gradient appears in the Y-direction (Fig. 2.8) if a thermal current flows in the X-direction and a magnetic field is applied in the Z-direction. Nerst Voltage is given by the relation.

$$V_N = QB \frac{dT}{dx}$$

where $Q = \text{Nerst Coefficient}$

$\frac{dT}{dx}$ = temperature gradient along x.

At temperature T , Q is related to Etingshausen Coefficient P according to the relation

$$Q = \frac{PK}{T}$$

Where K is the thermal conductivity of the Hall element.

RIGHT-LEDUC EFFECT: Temperature gradient along Y-axis is produced, when a thermal current flows in the direction of x-axis and the magnetic field acts along Z-direction.

$$\frac{dT}{dy} = R_L B W_x \quad \text{where } W_x = \text{Heat current density in the X-direction.}$$

and $\frac{dT}{dy}$ = Heat current density in the y-direction

R_L = Right-Leduc Coefficient

PELTIER EFFECT: This phenomenon produces a temperature gradient

along the Hall element in which an electric current is flowing. Such a temperature gradient can also arise from a non-uniform dissipation of heat from the element or its surroundings. This temperature difference will cause a thermal current to flow along the length of the element. In the presence of such a thermal current, the Nernst effect and the Righi-Leduc effect would become prominent.

The first three effects are magnetic field dependent, whereas the last one is independent of the field and depends upon the current flowing and non-uniform heat distribution. For weak magnetic fields, the corresponding thermo-electric voltages will be very small and can be reduced by the use of heat sink. They can be compensated by the arrangement used in reducing the misalignment voltage.

(V) MAGNETORESISTANCE: Magnetoresistance affects the linearity of the Hall device when the magnetic field is measured over a wide range. The input and output resistances of the Hall element are function of magnetic field for constant value of control current and temperature. The dependence of resistance upon magnetic field is called magnetoresistance effect. It is approximately proportional to the square of the product of carrier mobility and magnetic field intensity. (26)

(VI) TEMPERATURE EFFECT: The Hall output is affected by the changes in the temperature. The heat generated in the Hall element in the absence of heat sink will raise the temperature of the element, the parameters of the Hall element will change, thus affecting the sensitivity of the Hall element. These changes in sensitivity are introduced due to the fact that the Hall Coefficient is temperature dependent.

Various output and input circuits (27), (28), (29) consist-

ing of parallel combination of a thermistor and zero-temperature Coefficient resistance, placed in series with the Hall generator have been employed to reduce the temperature dependence of the Hall Coefficient.

All these methods lead towards lower sensitivity. It is also possible that the network may fail to follow small temperature variations experienced by a Hall generator of small size.

In the following the temperature stability is analysed and we will examine the possibility of increasing stability by the proper choice of material and dimensions of the Hall element.

Voeikov (30) defined the coefficient of stability K as the ratio of open circuit Hall voltage per Gauss to one half the voltage between the current terminals of the Hall probe.

From Eq. 2.5, we have

$$\frac{V_H}{B} = \frac{R_H}{t} I F\left(\frac{l}{b}\right) 10^{-8}$$

V_{13} = one half voltage between control current terminals

$$= \frac{1}{2} I R_i = \frac{1}{2} I \frac{\rho l}{bt} = \frac{1}{2} \frac{I l}{bt} \frac{R_H}{\mu}$$

where ρ = resistivity of the material = $\frac{1}{ne\mu}$

μ = mobility of the carrier

R_H = Hall constant = $\frac{1}{ne}$

n = Carrier concentration

K = Coefficient of stability

$$= \frac{\frac{V_H}{B}}{V_{13}} = \frac{1}{2} \frac{b}{l} \mu F\left(\frac{l}{b}\right) 10^{-8} \dots\dots\dots 2.8$$

For the same Hall element geometry, the stability coefficient is proportional to mobility. A high mobility material will be selected as

the best choice for the Hall element. K depends on dimensions b and l in a complicated way as shown in Eq. 2.8. Its effect will be examined in the section on "Choice of material."

(VII) NOISE

Thermal, current, flicker and contact noise will be considered.

THERMAL NOISE

Hall effect device is a two port passive device. Any noisy two port can be replaced by a noiseless two port and two noise voltage sources, one at the input and one at the output as shown in Fig. 2.9.

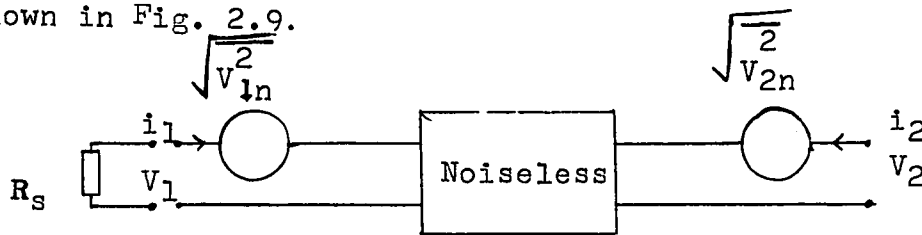


Fig. 2.9

$$V_1 = R_{11} i_1 + R_{12} i_2$$

$$V_2 = R_{21} i_1 + R_{22} i_2$$

$$\overline{V_{1n}^2} = 4 kTR_{11} \Delta f$$

$$\overline{V_{2n}^2} = 4 kTR_{22} \Delta f$$

where R_s is the source resistance, k the boltzmann's constant, T the absolute temperature and Δf the bandwidth.

The noise voltages at input and output are uncorrelated

when $R_{12} = - R_{21}$

Under this condition, the lowest value of the noise figure of a

Hall element of 7.66 db is obtained (31) if $R_{11} = R_{22} = R_{21}$

For $R_{12} = R_{21}$ the total noise voltage at the output is

$$\sqrt{4k T \Delta f \left(\frac{R_{21}^2}{R_s + R_{11}} + R_{22} + \frac{2 R_{12}^2}{R_s + R_{12}} \right)}$$

The third term is the result of correlation between the input noise voltage and the output noise voltage.

CURRENT NOISE: This noise is caused by current fluctuations that arise from randomly fluctuating emission of charge carriers. Consider a Hall element of concentration 5×10^{14} carriers per CC and dimensions:

Length = .508 cm

Width = .254 cm

Thickness = .0076 cm

Volume = $98 \times 10^{-5} \text{ cm}^3$

average No. of carriers = $\bar{N} = 98 \times 10^5 \times 5 \times 10^{14}$
 $= 4.9 \times 10^{11}$

average transit time = $\bar{\tau}_0 = \frac{\bar{N}e}{I} = \frac{4.9 \times 10^{11} \times 1.6 \times 10^{-19}}{50 \times 10^{-3}}$

where $I = 50 \text{ mA}$ is taken

$\bar{\tau}_0 = 1.57 \times 10^6 \text{ sec}$

In a semiconductor $\bar{\tau}_0 \gg \tau$, where τ is average life time of a carrier. Hence, the mean square noise current i_n^2 may be computed according to Guggenbuehl's formula (31)

$$\bar{i}^2 = \frac{4I^2 \tau_1 \tau_2^2 \Delta f}{N (\tau_1 + \tau_2)^2 (1 + w^2 T^2)}$$

where I = current through Hall element

τ_1 = average life time of a carrier

τ_2 = average life time of a trapped carrier

For $\omega T \ll 1$ (low frequencies)

$$\tau_1 = 10^7 \text{ sec}$$

$$\tau_2 = 10^8 \text{ sec.}$$

$$I = 50 \text{ mA}$$

$$\overline{i^2} = 2.04 \times 10^{-23} \Delta f$$

The mean square noise voltage developed across the output resistance of Hall element = $\overline{i^2} \times R_0^2$

let $R_0 = 100 \Omega$ (A typical value for polycrystalline In sb at liquid nitrogen temperature)

$$\text{Current noise voltage} = 4.5 \times 10^{-11} \sqrt{\Delta f} \text{ Volts}$$

$$\begin{aligned} \text{Thermal noise voltage of } 100 \Omega &= \sqrt{4kT \times 100 \Delta f} \\ &= 6.44 \times 10^{-9} \sqrt{\Delta f} \text{ Volts} \end{aligned}$$

It is clear that current noise is much smaller than the thermal noise and it can be neglected.

FLICKER NOISE: This noise is also called "excess noise" or " $\frac{1}{f}$ noise".

The last name describes one of its most characteristic features. The mean square voltage fluctuations have a spectral density of the form $\frac{1}{f}$. This spectral shape has been observed on different semiconductor devices from 5×10^{-5} cycles well up into the megacycles. Generally, in a sample, the noise current is found to be proportional to the square of the direct current I. This leads to the conclusion that pure conductivity fluctuations prevail. (32)

$$\text{So } \frac{\overline{i_f^2}}{I^2} = \frac{(\Delta \delta)^2}{\delta^2}$$

where σ = Conductivity of the material

The modulation of conductivity can thus be attributed to fluctuations of carrier density. The mechanism of this noise is not fully understood, although surface and volume properties appear to be important in determining its magnitude.

CONTACT NOISE

The properties of the Hall plate contacts play an important role in the operation of the device. If the contacts are not ohmic, the rectification, whether by the control current or Hall contacts leads to considerable noise in the output. The degree of rectification is strongly affected by the contact form and it is therefore desirable that the contact area should be large so as to reduce the amount of rectification. Soldering of contacts should be done by a low melting point solder in order to reduce the possibility of introducing inhomogeneity in the material.

2.4 CHOICE OF MATERIAL

For low level magnetic field measurements, the choice of the Hall material depends upon the following requirements:

1. large open circuit Hall voltage.
2. large ratio of Hall voltage to noise.
3. independence of temperature within the working range.

Keeping in mind these basic requirements, we will investigate the suitable material for the present work. The open circuit Hall voltage is given by Eq. 2.5

$$V_H = F \left(\frac{b}{b}\right) \frac{R_H}{F} I B \times 10^{-8} \text{ volts}$$

Our main concern is to maximize the expression:

$$\frac{V_H}{B} = F \left(\frac{l}{b}\right) \frac{R_H}{t} I \times 10^{-8} \dots\dots\dots 2.9$$

for the given input power.

The power supplied to the Hall element is

$$W = I^2 R_i$$

where R_i = Input Resistance = $\frac{\rho l}{bt}$

where ρ is the resistivity of the material.

$$\text{Thus, Input power} = W = \frac{I^2 \rho l}{bt}$$

or

$$I = \left(\frac{Wbt}{\rho l}\right)^{\frac{1}{2}} \dots\dots\dots 2.10$$

Combining Eqs. 2.9 and 2.10, we have

$$\frac{V_H}{B} = F \left(\frac{l}{b}\right) \frac{R_H}{t} \left(\frac{Wbt}{\rho l}\right)^{\frac{1}{2}} \times 10^8 \text{ volts/Guass.} \dots\dots\dots 2.11$$

$$\text{Since } \rho = \frac{1}{ne\mu}$$

where n = Carrier concentration /cc

e = electronic charge in coulomb

μ = mobility of the carrier in sq-cm/V-sec

$$\text{and } R_H = \frac{3\pi}{8} \frac{1}{ne} = \frac{3\pi\mu\rho}{8} \quad (\text{Hall constant for a semiconductor})$$

Introducing the values of R_H and ρ in eq. 2.11, we have

$$\frac{V_H}{B} = F \left(\frac{l}{b}\right) \left(\frac{3\pi}{8} \frac{wb}{t}\right)^{\frac{1}{2}} (\mu R_H)^{\frac{1}{2}} 10^8 \text{ Volts/Guass} \dots\dots\dots 2.12$$

Eq. 2.12 states that for material of similiar geometry and equal power dissipation, the figure of merit is

$$(\mu R_H)^{\frac{1}{2}}$$

In order to obtain a large Hall valtage, the carrier mobility and Hall coefficient should be large. In table 2.2 (19) are

TABLE 2.2

Material	Temp. K ^o	Electron Mobility	Resistivity (Ω -cm)	Hall Coefficient	(μR) ^{$\frac{1}{2}$}
In Sb	78	580,000	0.107	62,000	189,600
In Sb	78	400,000	0.09	39,000	125,000
In Sb	78	460,000	0.05	27,000	112,300
Si	78	10,000	50.00	500,000	70,050
In As	78	75,000	.009	650	6,980
Ge	298	3,600	25.0	87,000	17,700
Si	298	1,700	100.0	170,000	17,000
In As	298	36,000	0.0173	600	4,640
In Sb	298	60,000	0.005	350	4,600
GaAs	298	8,500	0.2	1,700	3,570
In AsP	298	10,500	0.08	850	2,985
Si	298	1,500	1.5	2,250	1,836
In sb	298	25,000	0.0035	100	1,580

given the characteristics of a number of semiconductor materials, where the figure of merit is calculated at room temperature and also at liquid nitrogen temperature.

Indium Antimonide fulfills the requirement of high mobility and large Hall Coefficient at liquid nitrogen temperature and is therefore considered most suitable material for the present work.

Its low resistivity as compared with other semiconductor materials at the same temperature, keeps the input and output impedances of the Hall generator at a low value. Low input impedance allows us to pass more control current for a particular input power, to obtain higher Hall output. Low output impedance reduces the thermal noise and thus increases the signal to noise ratio.

Although silicon and germanium have the highest merit figure of 17,000 and 17,700 respectively at room temperature, input impedances are quite high as compared to Indium Antimonide probe of the same dimension. Due to high input impedance, the control current through these materials is small compared with the Indium antimonide probe of the same dimensions. The merit figure of silicon is nearly half that for Indium Antimonide at liquid nitrogen temperature. This suggests that the use of silicon is not recommended as probe material for the present work.

TEMPERATURE DEPENDENCE OF HALL COEFFICIENT: Full utilization of high value of Hall Coefficient is prevented by the large temperature coefficient of sensitivity. The temperature dependence of Hall Coefficient can be reduced by doping the material with a particular impurity concentration. Impurity concentration will increase the carrier concentration, thus decreasing the Hall

Coefficient and hence the sensitivity. Thus what is gained in terms of stability against temperature changes, is lost in terms of sensitivity.

In view of these considerations, and keeping in mind the main purpose of achieving the higher sensitivity the Hall element should be maintained at liquid nitrogen temperature. This liquid serves as a constant temperature bath and the condition of constant heat removal is satisfied.

It is experimentally observed that Hall Co-efficient of Insb remains constant over a range 120° K to 70° K. (33), (19). This fact shows that temperature dependence of Hall Coefficient can be eliminated by operating the Indium Antimonide Hall probe at liquid nitrogen temperature (78°K).

CHOICE OF DIMENSIONS: The open circuit Hall voltage varies as $(\frac{b}{tL})^{\frac{1}{2}} F(\frac{L}{b})$ as shown in equation 2.12. For fixed heat removal, this term should be maximum.

In the first instance, the length and breadth of the element are taken into account and their combined effect on this term is considered. The effect of thickness is examined later.

The factor $(\frac{b}{tL})^{\frac{1}{2}} F(\frac{L}{b})$ is computed for various values of length to breadth ratio and is shown in table 2.3. The values of $F(\frac{L}{b})$ are taken from table 2.1.

The maximum value of the term $(\frac{b}{tL})^{\frac{1}{2}} F(\frac{L}{b})$ occurs when the ratio $\frac{L}{b}$ is chosen around 1.5. This optimum value is in agreement with the result from theoretical considerations by Lofgren (34).

For values of $\frac{L}{b}$ smaller than 2, shorting effect of current electrodes reduces the Hall Voltage (35). We choose

$$\frac{L}{b} = 2$$

TABLE 2.3

$\frac{d}{b}$	$F\left(\frac{d}{b}\right)$	$\left(\frac{b}{d}\right)^{\frac{1}{2}} F\left(\frac{d}{b}\right)$
3	.98	.565
2	.92	.650
1.5	.88	.715
1	.72	.72
.5	.50	.706
.25	.28	.56

The temperature stability as shown by Eq. 2.8, is proportional to $\left(\frac{b}{d}\right) F\left(\frac{d}{b}\right)$. This factor increases with the decrease in $\frac{d}{b} F\left(\frac{d}{b}\right)$. But for values of $\frac{d}{b}$ less than 2, sensitivity decreases due to shorting of current electrodes. Ratio $\frac{d}{b} = 2$ is chosen for higher sensitivity and moderate stability.

Since V_H is proportional to $\frac{1}{\sqrt{t}}$ as shown in Eq. 2.12, output can be increased by making the element thinner. The lower limit of t is fixed by fabrication problems and consideration of power dissipation.

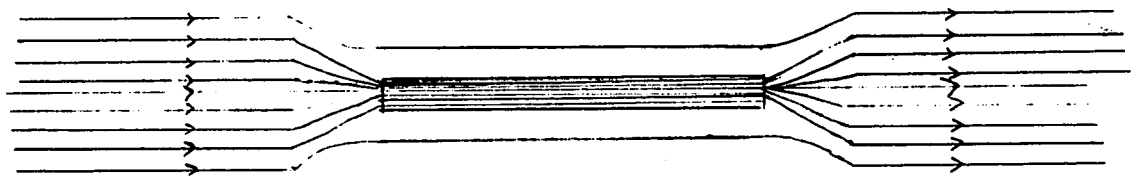
CHAPTER III

MAGNETIC FLUX CONCENTRATOR

3.1 INTRODUCTION

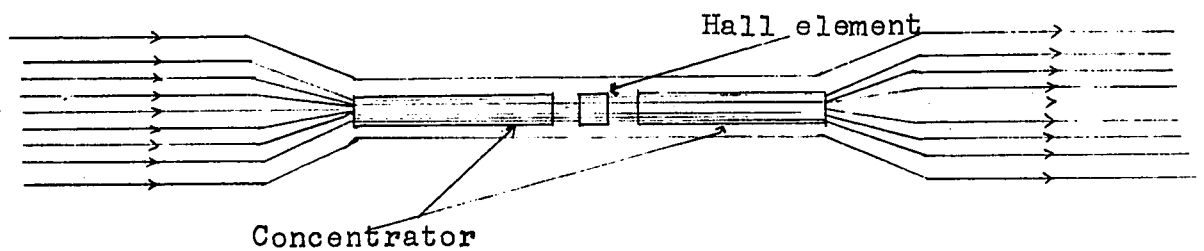
The sensitivity of the Hall probe can be greatly increased by placing it between the two high permeability rods, which increase the magnetic flux density acting on the Hall element. (19) (36).

The idea of a magnetic flux concentrator is illustrated in Fig. 3.1

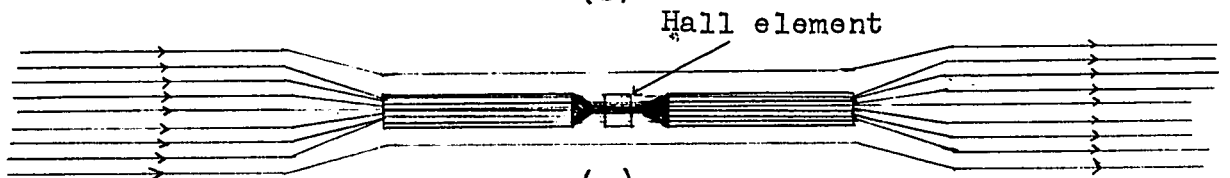


Lines of flux are denser inside the magnetic material than that out side.

(a)



(b)



(c)

Fig. 3.1

Any high permeability material when placed in a magnetic field, causes a deformation of the field pattern. The lines of flux try to follow the path of lower reluctance and thus the field

is distorted. Fig. 3.1a shows the pattern of flux lines, when a high permeability rod is placed in a uniform magnetic field.

If a high permeability magnetic rod is cut in two, to place the Hall element between the two halves, the gap will experience a higher flux density than without the rods. This is illustrated in Fig. 3.1b.

Further increase in sensitivity can be achieved by tapering the concentrator at the location of the Hall element as shown in Fig. 3.1c.

Tapered concentrator is useful when a Hall element is employed because of the small area of the element. Since the Hall Voltage is directly proportional to flux density, the "gain" in magnetic flux density due to concentrator will increase the sensitivity to the same extent.

3.2 SELF DEMAGNETISATION: When a ferromagnetic material is placed in a magnetic field and magnetic induction exists due to the field present, a self demagnetisation effect is encountered. Consider a magnetic material, which is magnetized by the field H_a , N and S poles are produced and an external field is set up owing to the poles with flux lines going from the N to the S pole externally. Additional lines of force go from N to S inside the material, and a magnetic force exists in opposition to the magnetization force H_a . This self inflicted demagnetization influence is function of:-

- (1) applied field and intensity of magnetization.
- (2) shape or geometry of the specimen of the magnetic material.

Demagnetization factor of a cylindrical rod.

Net effective field strength acting is

$$H_e = H_a - N I_m \dots\dots\dots 3.1$$

where H_a = applied magnetic field in oersted

N = Demagnetization factor

I_m = intensity of magnetization

$$\text{since } B = H_e + 4\pi I_m \dots\dots\dots 3.2$$

combining Eqs. 3.1 and 3.2, we get

$$H_e = H_a - \frac{N}{4\pi} (B - H_e) \dots\dots\dots 3.3$$

Dividing Equation 3.3 by B, and taking the reciprocals on both sides we obtain,

$$\begin{aligned} \mu = \frac{B}{H_e} &= \frac{1}{\frac{H_a}{B} - \frac{N}{4\pi} (1 - \frac{H_e}{B})} \\ &= \frac{1}{\frac{1}{\mu_a} - \frac{N}{4\pi} (1 - \frac{1}{\mu})} \dots\dots\dots 3.4 \end{aligned}$$

where $\mu_a = \frac{B}{H_a}$ the apparent permeability.

For relatively high values of μ , $\frac{1}{\mu} \ll 1$

$$\mu = \frac{1}{\frac{1}{\mu_a} - \frac{N}{4\pi}} \dots\dots\dots 3.4a$$

$$\text{or } \mu_a = \frac{1}{\frac{1}{\mu} + \frac{N}{4\pi}} \dots\dots\dots 3.5$$

Values of N for different p (= $\frac{\text{length of the rod}}{\text{diameter}}$)

and K (susceptibility) were calculated, using the formula (37)

$$\frac{N}{K=\infty} = \frac{N}{EM} \frac{2.26 \ln(1+0.156)}{2.15 \ln(1+0.326)} + \frac{1}{1}$$

and $N_{K=0} = \frac{2\pi}{p^2}$

where $N_{Ell.}$ = Demagnetization factor of rotational ellipsoid

$$= \frac{4\pi}{p^2-1} \left[\frac{b}{\sqrt{p^2-1}} \ln (p + \sqrt{p^2-1}) - 1 \right]$$

TABLE 3.1

p	$N_{Ell.}$	$N_{K=0}$	$N_{K=\infty}$
10	0.2549	0.0628	0.193
12	0.1914	0.0442	0.143
15	0.1342	0.0279	0.1038
16	0.1188	0.0245	0.0915
18	0.1042	0.0194	0.081
20	0.0843	0.0157	0.0665
22	0.0695	0.0130	0.0551
25	0.0587	0.0100	0.0474

The demagnetizing factor depends upon the dimensions of the magnetic material. The higher is the ratio of the length of the magnetic rod to the diameter of its cross-section, the lower is the demagnetizing factor. In general the influence of demagnetizing factor is minimum for slender specimens and attains a maximum value when short length specimens of large area are encountered. For closed magnetic circuit, like a torus, $N = 0$, for a thin sheet or plate $N = 4\pi$

K the susceptibility is taken equal to infinity for high permeability magnetic material. ($\mu > 10,000$).

Consider an example of a rod of the following dimension:

length = 15.24 cm

diameter = .7 cm

then $p = \frac{\text{Length of the rod}}{\text{diameter}} = 22$

From table 3.1, we have for $p = 22$, $N = .0551$

Then the permeability of the rod = $\frac{1}{\frac{1}{\mu} + \frac{N}{4\pi}}$ Eq. 3.5
= 228 3.5a

Thus the flux density will be 228 times greater inside the magnetic rod than in the air. Further demagnetization occurs when the magnetic rod is split into two halves. An air gap is created to place the Hall element between the two halves.

Let us consider a magnetic rod in two halves, having an air gap of length l_g . (Fig. 3.2) Since flux lines are continuous, the flux in the gap will be equal to the flux in the magnetic material.

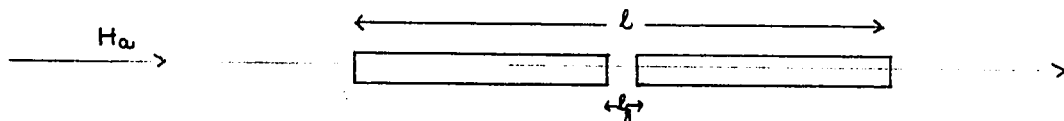


Fig. 2.3

From equation 3.1, we have

$H_e = H_a - N I_m$ 3.6

where N = self-demagnetizing factor due to air gap

I_m = intensity of magnetization

and $H_a l = H_e (l - l_g) + B l_g$

where B is the magnetic flux density inside the material

then $H_a = H_e \frac{l - l_g}{l} + B \frac{l_g}{l}$
 $= H_e + B \left(\frac{l_g}{l}\right) \dots\dots\dots 3.7$

since $l_g \ll l$

The flux density inside the material is

$B = H_e + 4 \pi I_m \dots\dots\dots 3.8$

Combining Eqs. 3.7 and 3.8, we have

$H_a = H_e \left(\frac{l + l_g}{l}\right) + 4 \pi I_m \left(\frac{l_g}{l}\right)$

or $H_e = H_a - 4 \pi I \left(\frac{l_g}{l}\right) \dots\dots\dots 3.9$

Comparing Eqs. 3.6 and 3.9, we have $N' = + 4 \pi \left(\frac{l_g}{l}\right) \dots\dots\dots 3.10$

For very small air gap $N' = 0$

The effect of demagnetization introduced by the air gap should be kept minimum, either by increasing l or decreasing l_g. Since we have to introduce the Hall element in the gap, the air gap length is fixed by the thickness of the Hall element.

In order to achieve the maximum magnetic gain determined by equation 3.5, N' should be negligible as compared with N.

For l_g = .005 cm, l = 15.24 cm

we have N' = .00516 from Eq. 3.10

This value of N' is nearby 10 times less than the particular value of N given by Eq. 3.5a. Further increase in gain is obtained by tapering the poles at the Hall element.

3.3 LEAKAGE FLUX

The most important one is the fringing flux which occurs

in the vicinity of the gap. It reduces the gap reluctance and increases the cross-sectional area of the face of the magnetic material.

Fringing flux decreases to a low value, when area to air gap length ratio is very large. Flux can be assumed to be uniform in an area $(l-l_g)(w-l_g)$ in case of a rectangular rod. (38)

In making the pole faces of the concentrator, the length and breadth of the pole faces should be increased by the length of the air gap (thickness of the Hall element), in order to obtain a uniform magnetic field on the Hall element.

CHAPTER IV

EXPERIMENTAL WORK

4.1 HALL ELEMENT

Hall element Beckman Model 335 was chosen as the magnetic field sensing device, having the following specifications:

Indium Antimonide thin film Hall element

Input Resistance = 135 ohms

Output Resistance = 52 ohms

Input power (Still air) = 125 mW

Sensitivity = 4.5 Volts/ampere-kilo gauss

Length of the Hall element = .2"

Breadth = .06"

Overall thickness = .04"

The selection was made in consideration of higher sensitivity required for this type of work, which resulted from small thickness of the film (.002") and utilization of ferrite substrate.

Introducing the value of sensitivity into Eq. 2.4a, Hall voltage is given by

$$V_H = 4.5 IB 10^3 \text{ volts}$$

where

I = control current in amperes

B = Magnetic field applied in gauss

For a control current of 25 mA, the open circuit Hall voltage due to the magnetic field of the order of 10^6 gauss is

$$1.25 \times 10^{10} \text{ volts}$$

The magnetic concentrator with a gain of about 200 increases the Hall voltage to 2.5×10^8 volts. Further increase in the Hall voltage can be obtained by passing more control

current with proper heat sink.

4.2 LOW NOISE AMPLIFIER

To measure the ultra low level signal, Astrodata Model 120 Nanovolt Amplifier having the following specifications was used

Gain	200 to 1,000,000
Input Resistance	1 M Ω
Frequency Response	dc to 100 cps (3db)
Noise referred to input	5.0 x 10 ⁻⁸ volts peak to peak dc to 1 cps. 25 x 10 ⁻⁸ volts peak to peak 1 cps to 20 cps, for source resistance of 100 ohms.

DC signal of .05 μ v can be detected with this amplifier.

4.3 PRODUCTION OF MAGNETIC FIELD

Uniform magnetic field is produced at the axial line AB of the Helmholtz coil by passing the current through the coil.

(Fig. 4.1). The coils have the following dimensions:

N_t = 130 turns in each coil

Radius = .15 meter

field strength at the axis of the coil is given by

$$H = \frac{8}{125} \frac{NI}{R} \text{ ampere turns/meter}$$

$$= \frac{8}{125} \frac{NI}{R} \quad 4\pi \times 10^3 \text{ oersted}$$

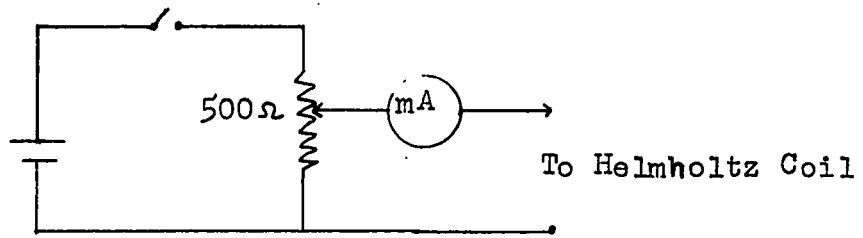
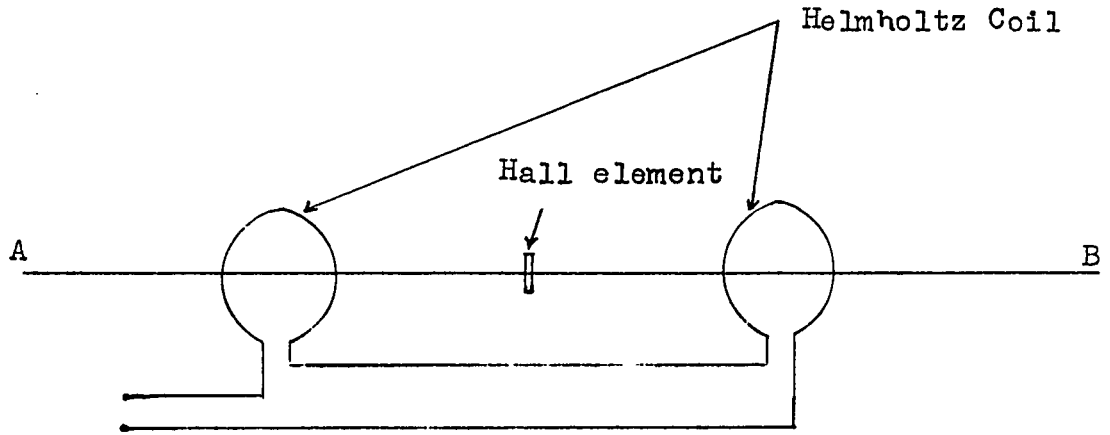
$$= 7.8 \times 10^3 \text{ oersted for 1 mA dc current through the}$$

coil.

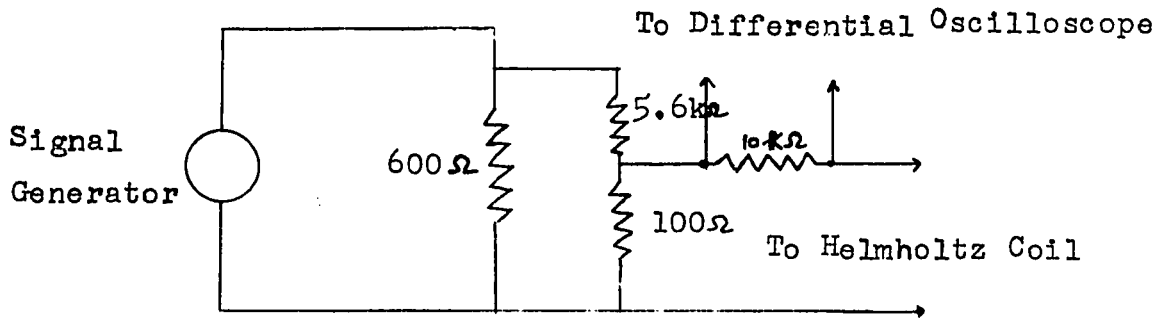
Circuit diagram for producing dc magnetic field is shown in

Fig. 4.1a.

Fig. 4.1b shows the arrangement for producing ac magnetic



(a)



(b)

Circuit diagram for producing (a) dc field (b) ac field

Fig. 4.1

field. Voltage is measured across 10 k Ω resistor by differential oscillo scope and current passing through the Helmholtz coil is determined.

4.4 MAGNETIC FLUX CONCENTRATOR

Thin laminations of mu-metal, permalloy-80 and mu-metal rods were used as magnetic flux concentrator. Mu-metal laminations of dimensions, length 1.5", breadth .25", thickness .014" and permalloy-80 of the following dimensions have been used.

Length = 1.5", 1.75", 2"

Breadth = .25"

Thickness = .006"

These dimensions in case of permalloy-80 gave us three different lengths (3", 3.5" and 4") for the flux concentrator to be used in combination with the Hall element.

The magnetic sensing area of the Hall element Model 335 is .2" x .06". The ends of the concentrator should be of the same dimensions for the optimum use of the concentrator. In order to have nearly the same area at the ends facing the Hall element, the laminations are tapered at these ends. The breadth of the laminations is fixed. The other variable dimension of the concentrator is the overall thickness which is varied by changing the number of the laminations.

Since the laminations were difficult to handle and keep them in contact, mumetal rod of cross-sectional diameter .28" is utilized as a magnetic flux concentrator at a later stage of the experiment.

Two pieces of 2.5" each were taken from the main rod. The ends facing the Hall element were made to have an area of 0.2" x 0.1"

and both pieces were annealed.

4.5 DESCRIPTION OF THE APPARATUS

Fig. 4.2 shows the set up to measure the magnetic gain of the apparatus and detect the unknown magnetic field.

(I) COMPENSATING NETWORK

Misalignment voltage and the output of the Hall element due to the ambient dc field is compensated by adjusting the various potentiometers shown in Fig. 4.3 over a wide range. The control current is supplied by two Mallory batteries (1.5 volts) and adjusted by the potentiometer P_1 . The control current flowing through the Hall element is measured by a milliammeter M.

(II) AMPLIFIER

Main features of the amplifier were described in the section 4.2. Gain settings are checked and found to be accurate. Input noise is found to be $0.1 \mu v$ peak to peak for a source resistance of 52 ohms in the frequency range dc to 25 c/s.

(III) 60 c/s REJECTION CIRCUIT

The lower level of measurement is influenced by noise from the Hall element, amplifier, voltage induced in the instrument leads and 60 c/s stray magnetic fields. The noise from the 60 c/s interference signal is considered here.

An ideal solution to this problem would be to have a filter with a unity gain, except at the frequency of the undesired signal, at which the gain should be zero.

Parallel Tee Network was constructed and is shown in Fig. 4.4. Matched capacitors and resistors are selected for the optimum performance of the filter. Filter response is shown in

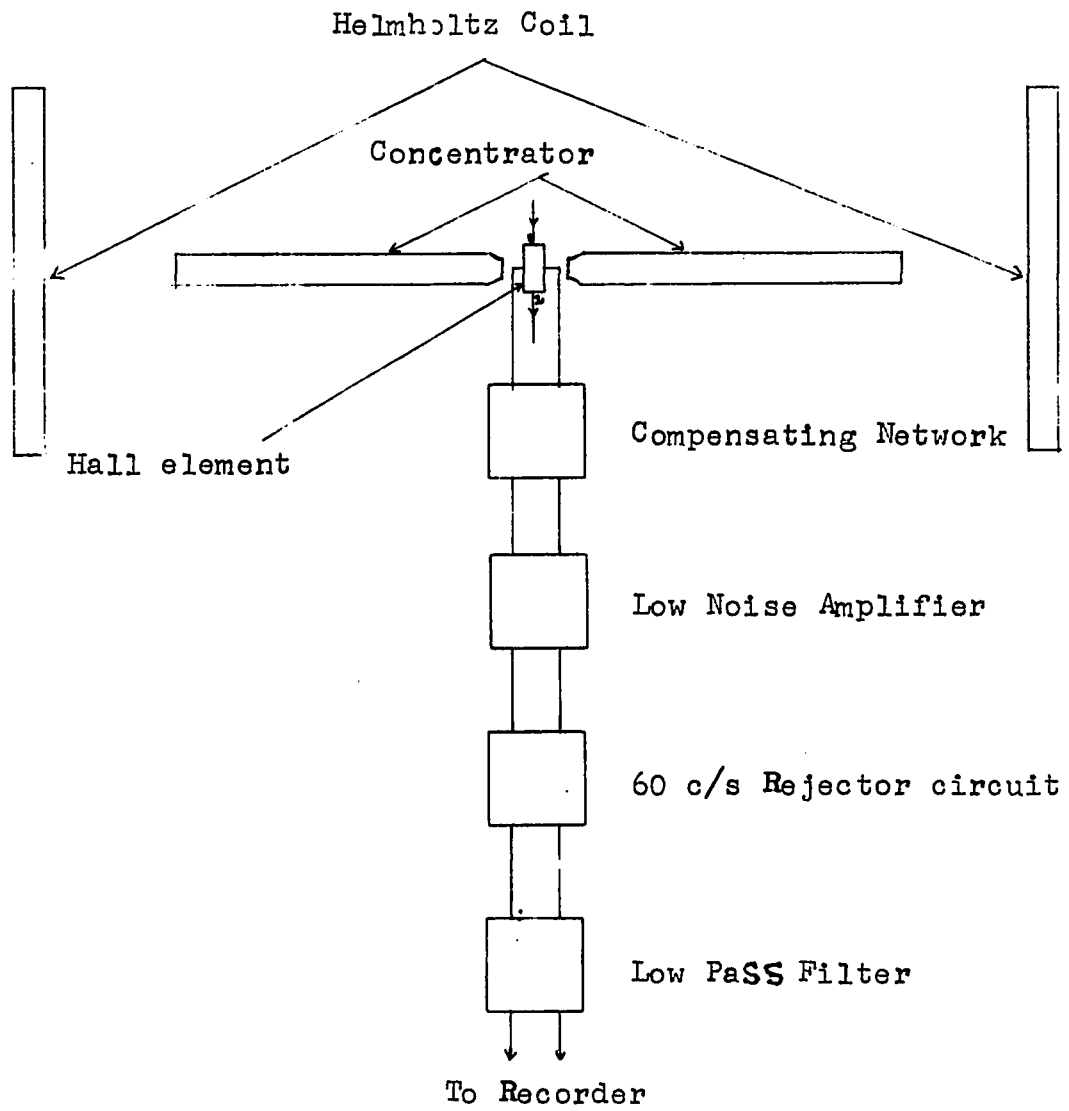


Fig. 4.2

Block diagram for measurement of the magnetic field and magnetic gain of the concentrator.

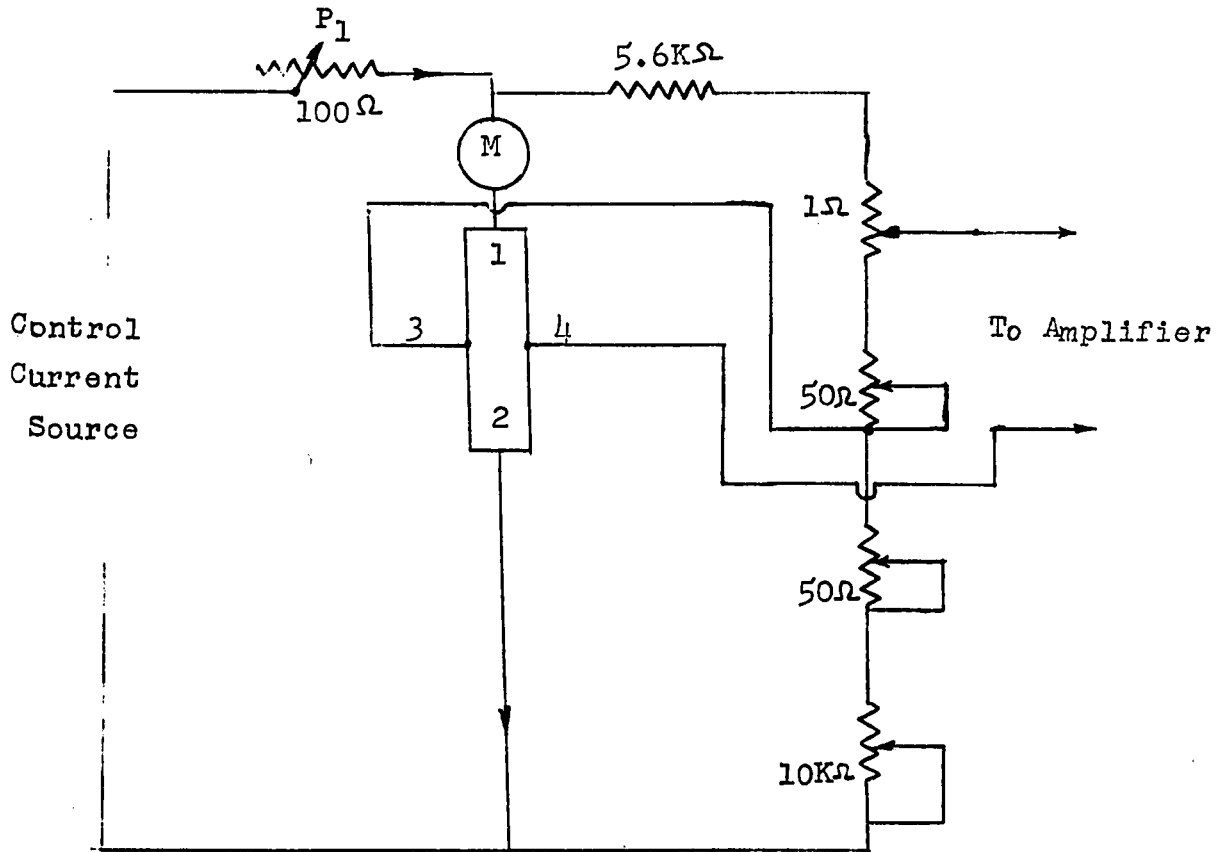


Fig. 4.3

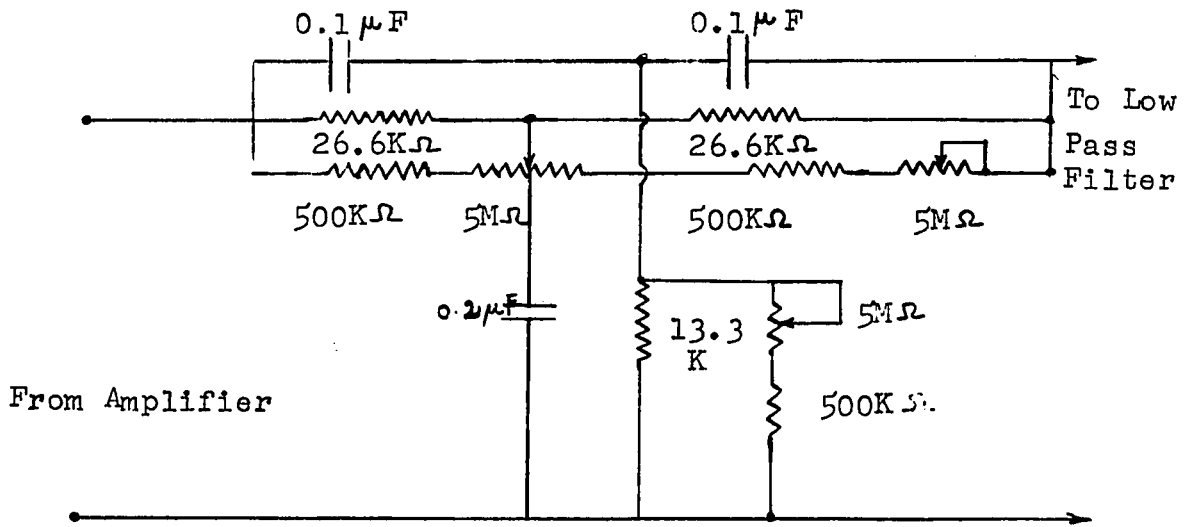


Fig. 4.4

Fig. 4.5 Response curve of 60 c/s
Rejection circuit.

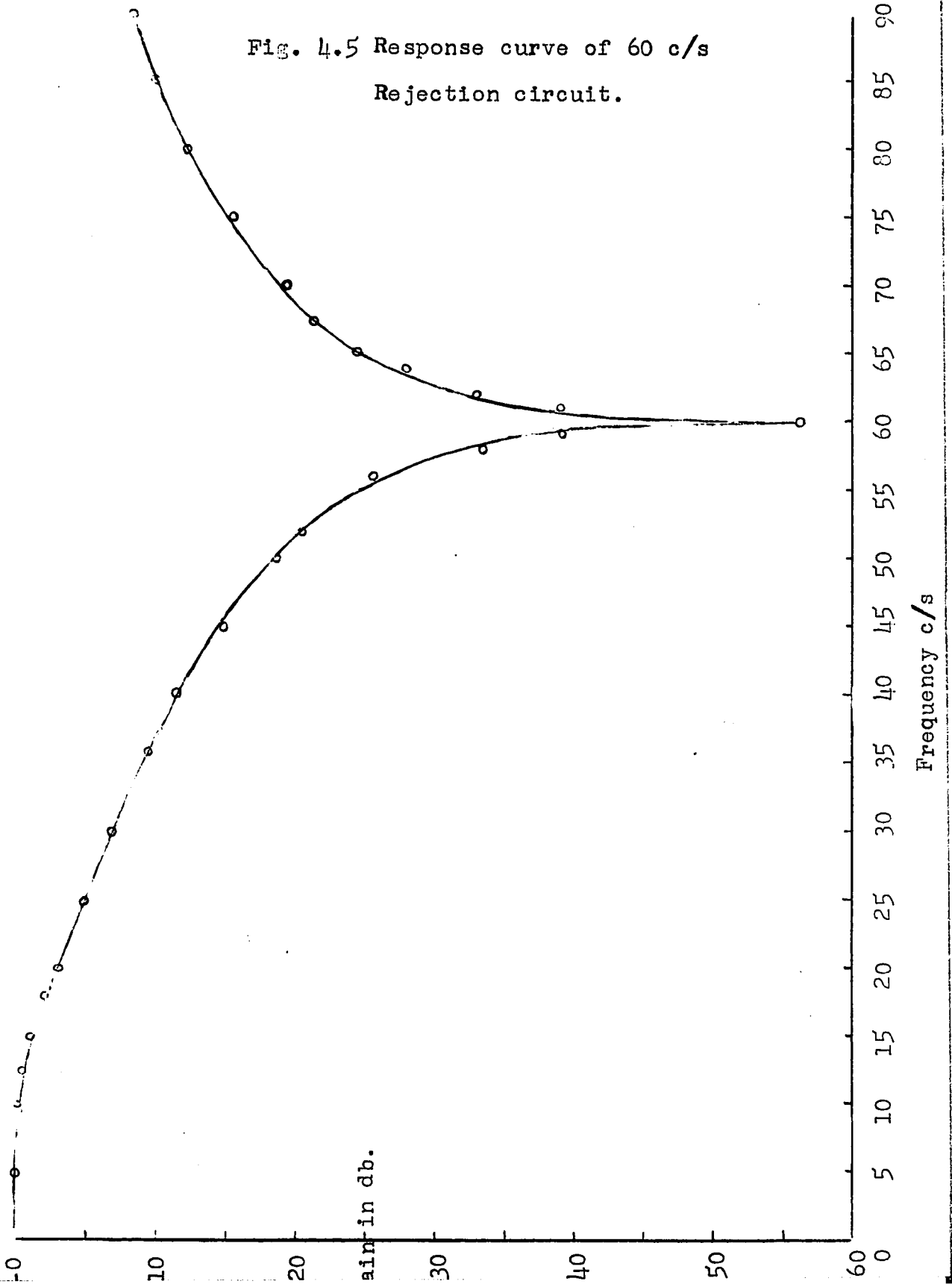


Fig. 4.5. Attenuation at 60 c/s interference signal is 56 db. The response falls to 3 db at 20 c/s, giving a frequency response flat within 3 db from dc to 20 c/s.

(IV) LOW PASS FILTER

In order to avoid the high frequency pick up and also to minimize the noise of the amplifier by limiting the bandwidth a low pass Spectrum Analog Filer Model LH - 24 is employed.

(V) RECORDER AND MICRO VOLTMETER

For dc measurements Kiethly Micro Voltmeter Model 150 A and Hewlett Packard Micro Voltmeter having 2% measurement accuracy are employed. Brush Recorder, Mark 11, is used for ac measurements.

4.6 OPERATION

25 mA dc control current was passed through the Hall element, which is placed between two brass rods. The brass rods reduce the temperature variations inside the Hall element and help to keep the element at a fixed position.

Output of the Hall element was reduced to zero by adjusting the compensating network in the absence of the applied field. Known current was allowed to flow through the Helmholtz coil, thus producing a known perpendicular field at the Hall element. Output was noted for different values of magnetic field. A linear relation was found between the Hall output and the magnetic field by plotting on a graph paper.

An insulated mounting base for keeping the laminations intact was made and Hall element was placed between the tapered ends of the laminations. Output was noted for the same values of the

magnetic field. The graph between output and magnetic field showed a linear relation between these quantities. Magnetic gain of the concentrator was measured from these two graphs.

4.7 MAGNETIC GAIN OF THE CONCENTRATOR

Magnetic gain of mumetal laminations concentrator of 3" length was found to be 105. Concentrator of permalloy-80 laminations, of length 3", 3.5" and 4" produced a magnetic gain of 104, 135 and 180 respectively. All these observations were carried with the Hall element Model 335.

It was also observed that the thickness of the concentrator plays an important role in determining the magnetic gain. The optimum value of the thickness occurred in the neighbourhood of 64 laminations, which gave the equivalent diameter of the concentrator to be 0.4" (1 cm nearly).

Permalloy rod of diameter .7 cm was also utilized instead of laminations. The magnetic gain of this 5" long concentrator was found to be 210. This unit was selected for further work due to its high gain, easy handling and good thermal contact with the Hall element.

4.8 TEMPERATURE EFFECTS

The Hall element is found to be temperature dependent. The temperature dependence of Hall coefficient changes the sensitivity, thus introducing error in the measurement. Zero field signal level or zero balance shifts with the changes in temperature. It is desirable that zero adjustment should not change during the experiment. Some stability can be achieved

through the use of heat sink for the Hall element, control of ambient temperature and shielding the probe assembly from air currents.

In order to obtain the temperature stability, the mounting base for the concentrator was made of brass which provided good thermal contact with the Hall element and the concentrator. The temperature gradient in the plate was further minimized by coating the plate with a layer of silica loaded grease. This helped to minimize the uneven heat dissipation in the Hall element. The whole probe assembly was insulated from circulating air current. All these precautions led to the stability of the zero balance less than $1\mu\text{v}$ for a control current of 25 mA.

4.9 NOISE

Noise superimposed on the zero balance in the frequency range of low pass filter was observed when the gain of the amplifier was increased. This was found to be 18 times higher than the amplifier input noise. This voltage was found to be of the same order of magnitude in all four samples of Hall element which were used in the experiment. Using all the precautions mentioned in the section 4.8, the noise voltage was found to be $0.9\mu\text{v}$ peak to peak with the concentrator of magnetic gain 210 at the room temperature. Noise voltage increased to $11\mu\text{v}$ peak to peak when the Hall element without silicon grease was operated in open air and was not prevented from circulating air currents. Passing vehicles on the nearby road and the vibrations in the probe assembly also increased the noise voltage. Observations were

taken usually at night when the interference from the surroundings was reduced.

In order to know the cause of fluctuations in the Hall output, the element was operated with brass rods, thus reducing the external effects by 210 times the gain of the concentrator. The noise voltage was found to be of the same order, showing that it was originating inside the Hall element.

Considering that it might be due to the thermal changes in the Hall element, the whole assembly was dipped in oil, but no improvement was observed.

In order to observe the temperature changes in the Hall element, an iron -constantan thermocouple junction was attached to one output terminal at a point where it just emerged from ferrite substrate. The hall element was placed between two brass rods mounted on a brass base. The whole assembly was enclosed in a large thermoflask to avoid the circulating air currents. 25 mA dc control current was allowed to flow through the Hall element. 30 minutes were allowed to reach the thermal equilibrium. The output of the thermocouple was amplified and observed on an oscilloscope. The output showed no variations as observed in the Hall output.

In order to see whether it is possible to reduce the noise and pass more control current, the Hall element was operated at liquid nitrogen temperature. It resulted in low sensitivity and marked increase in noise voltage. It gave a noise voltage of $6\mu v$ peak to peak for a control current of 5 mA. In spite of

the fact that $\frac{1}{5}$ th of the previous control current (25 mA) was flowing in the Hall element, the noise voltage increased nearly 6 times the previous value of $0.9\mu\text{v}$ at the room temperature. It was not considered feasible to pass more current, since noise increased markedly.

At liquid nitrogen temperature, the input resistance of the Hall element increased six times in comparison to its value at room temperature. The non-linear misalignment voltage also increased due to increase in resistivity of the Hall element. The changes in this component due to resistivity fluctuations produced the variations in the carrier concentration, thus producing the fluctuations in the Hall output. Marked increase in noise voltage at liquid nitrogen temperature may be attributed to the non-ohmic contacts. To detect the low level magnetic field, these factors must be taken into consideration.

A magnetic field of 4.0×10^5 gauss peak value was detected by operating the Hall element Model 335 at room temperature in combination with concentrator of magnetic gain 210. The detection of the signal lower than 4.0×10^5 gauss was corrupted by the presence of the noise voltage.

Further improvements in the measurement sensitivity of the device were sought in the fabrication of the Hall element of high sensitivity and low zero field noise. It was decided to use Indium Antimonide as a material at liquid nitrogen temperature as outlined in the 2nd chapter under the section of "choice of material."

4.10 PREPARATION OF HALL ELEMENT

The material was supplied by Asarco Intermetallics Corporation through their parent plant in England. The material selected was of type:

1. Single crystal N-type undoped
2. Polycrystalline N-type undoped

The material was in the form of ignots section of 0.175" thickness. The single crystal was in circular form of 1.2" diameter, whereas the polycrystalline was in semicircular in cross-section of 1.2" semicircular width. Both sample were of the same thickness. Slices of thickness nearly 40 mils were cut from the material. Difficulty was experienced while cutting with the diamond saw, due to the brittleness of the material. Chips from the sides came out as the material was cut. The wastage of the material was high, so this method was abandoned. The material was finally cut by motor driven fine stainless steel wire under pressure. Corborundum powder with water was applied during cutting process. This method was found ideal for cutting this brittle material.

The breadth-wise edges of the slice were then lapped to to make both edges parallel. The distance between the two parallel edges determined the width of the Hall element.

Again the slice was cut length-wise into pieces of the dimensions slightly longer than the length of the Hall plate. The length-wise edges were lapped to make them parallel and of exactly equal to the length of the Hall element. The

lapping along the edges helped the material from cracking during the last part of fine thickness lapping. It was experienced that for unlapped edges, cracks appeared when the pieces were lapped down to .004" thickness. The pieces were finally lapped to 0.003" thickness. They can be lapped to still lower thickness, but the handling of the samples becomes difficult and there is always danger of cracking the samples.

These samples were put in the acetone while they were still on the mesh plate of the lapping machine for at least 24 hours. Sometimes they had to be kept in acetone for 48 hours, so that they could be removed from the mesh plate.

The samples were then mounted on a permalloy-80 laminations by using a fine layer of epoxy. The epoxy serves a good thermal contact and electrical insulation. It takes a long time to dry up, otherwise there is always a possibility of cracking the brittle material. Later on, another method was adopted. The sample was mounted on a lamination by using one layer of cigarette paper and fine layer of nail varnish and it was found to withstand the liquid nitrogen temperature. The contacts were made using indium as a solder and zinc chloride as a soldering flux. Control current leads were soldered along the whole width of the Hall plate and Hall output terminals were made point contact. Each contact was viewed under high power microscope. Then the sample was washed in distilled water to dissolve the traces of zinc chloride. A thin layer of nail varnish was applied to cover the upper surface of the Hall element.

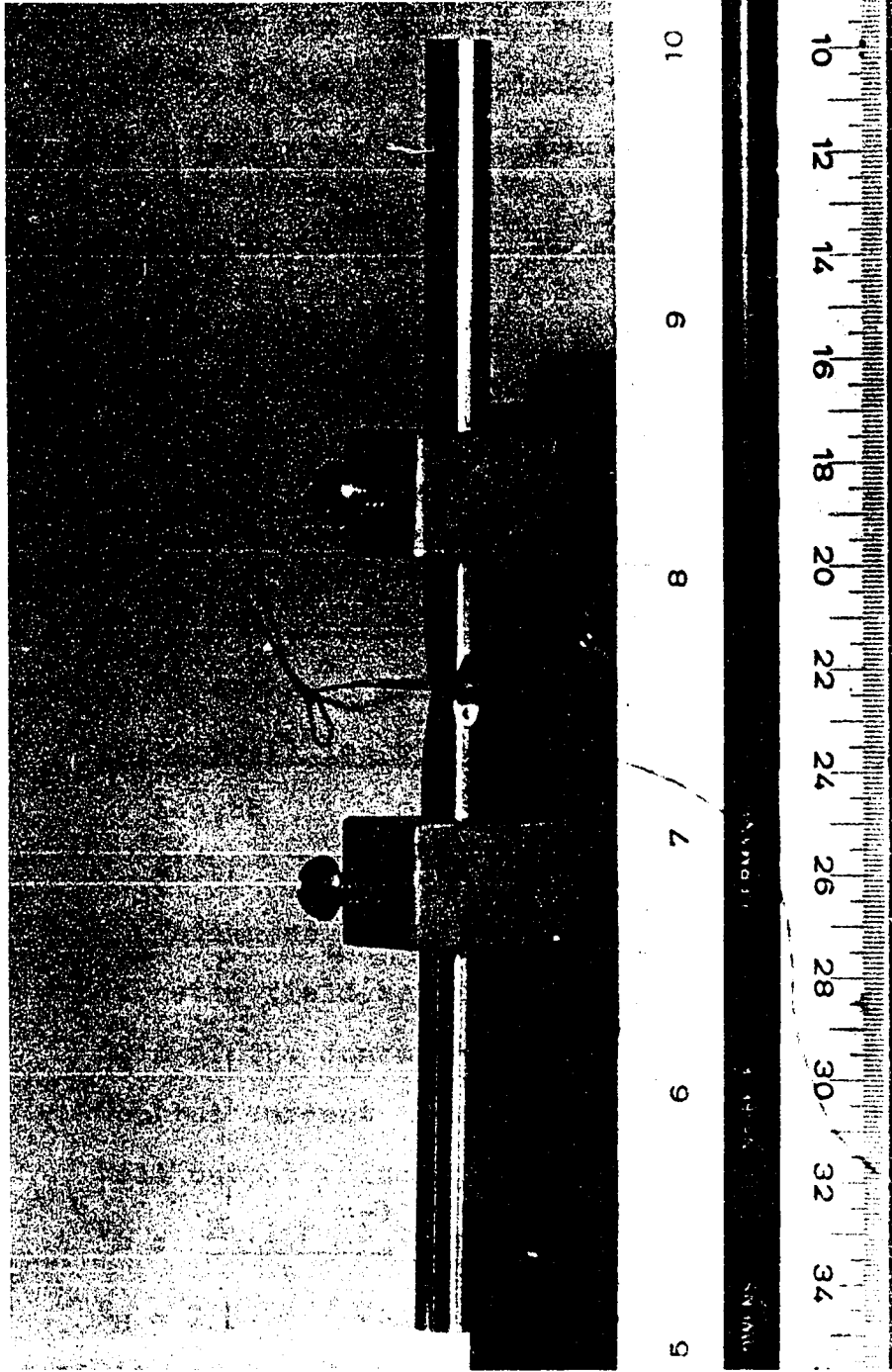


Fig. 4.6 Hall element with concentrator.

The contacts were checked on transistor curve tracer and found to be ohmic over the operating ranges of current.

The Hall element was placed between the concentrator, the ends of the concentrator just touching the sides of the element. (Fig. 4.6)

4.11 RESULTS

Magnetic gain of the concentrator at room and liquid nitrogen temperature was measured to be 202 and 100 respectively. The loss in gain at liquid nitrogen temperature might be due to the gap created between the element and the concentrator. The rods could not be pressed hard due to the danger of cracking the element. The maximum gain of 100 at liquid nitrogen temperature was obtained with 5" long concentrator.

Polycrystalline element at room temperature

Length = 0.2"

Width = 0.1"

Thickness = .003"

Magnetic field applied = 7.8×10^3 Gauss

Gain of the concentrator = 202

Control current = 40 mA

Hall output voltage = $V_H = 11 \mu v$

$V_H = \frac{R_H I B}{t} 10^{-8}$ Volts

$R_H = 133 \text{ cm}^3/\text{Coulomb}$

Sensitivity of the Hall element = .174 Volts/ampere -kilo gauss

Zero field noise Voltage = .2 μv peak to peak (Fig. 4.7)

With this arrangement, magnetic field strength of 1.5×10^4 gauss

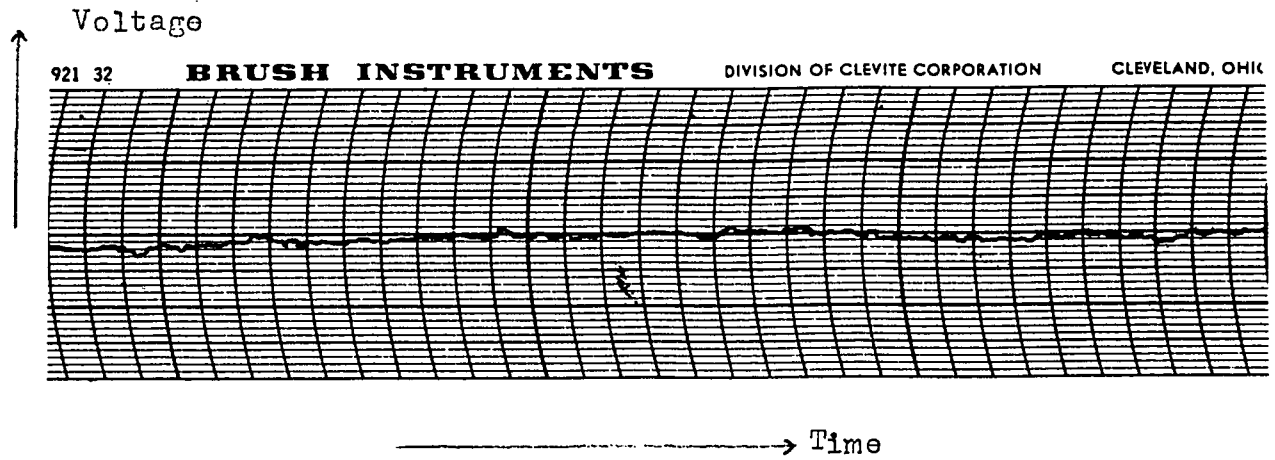


Fig. 4.7 Noise voltage = $.2\mu\text{v}$ peak to peak.
Control Current = 40 mA.
Bandwidth = dc to 25 c/s.
1 Small Chart Line = $.1\mu\text{v}$.

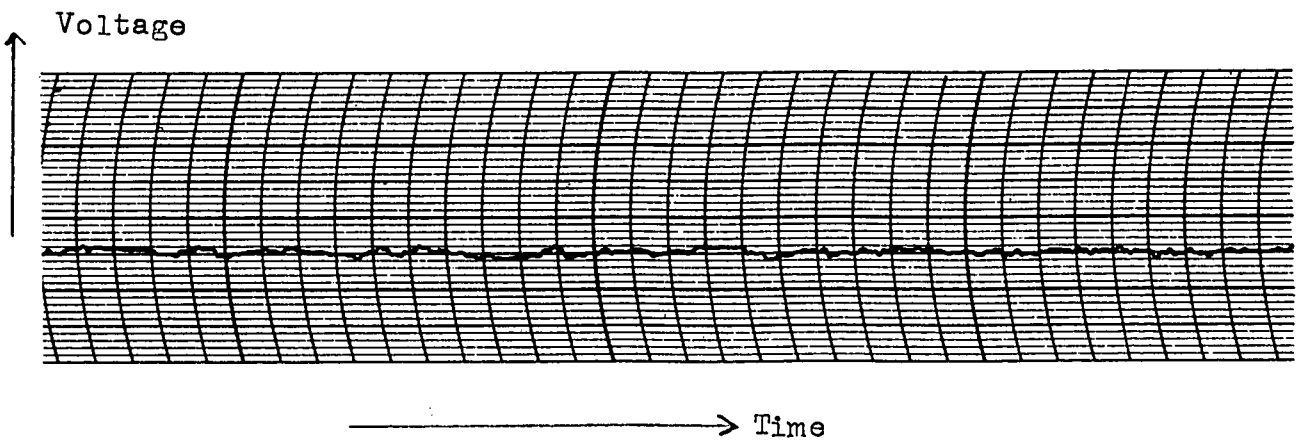


Fig. 4.8 Noise Voltage = $.1\mu\text{v}$ peak to peak.
Control Current = 50 mA.
Bandwidth = dc to 25 c/s.
1 Small Chart Line = $.05\mu\text{v}$.

peak value can be detected.

SINGLE CRYSTAL AT ROOM TEMPERATURE

Length = 0.2"

Width = 0.1"

Thickness = 0.003"

Magnetic field applied = $7.8 \cdot 10^{-3}$ Gauss

Gain of the concentrator = 202

Control current = 50 mA

Hall output voltage V_H = $17 \mu v$

Hall Coefficient R_H = $164.5 \text{ cm}^3/\text{Coulomb}$

Sensitivity of the Hall element = .2158 Volts/ampere - kilo gauss

Zero field noise voltage = $.1 \mu v$ peak to peak (Fig. 4.8)

Signal strength of 5.6×10^{-5} Gauss peak value can be detected
with this element.

POLYCRYSTALLINE MATERIAL AT LIQUID NITROGEN TEMPERATURE

Input Resistance = 121 ohms

Control Current = 10 mA

Input power = 12.1 milliwatts

Magnetic field applied = 7.8×10^{-3} Gauss

Gain of the concentrator = 100

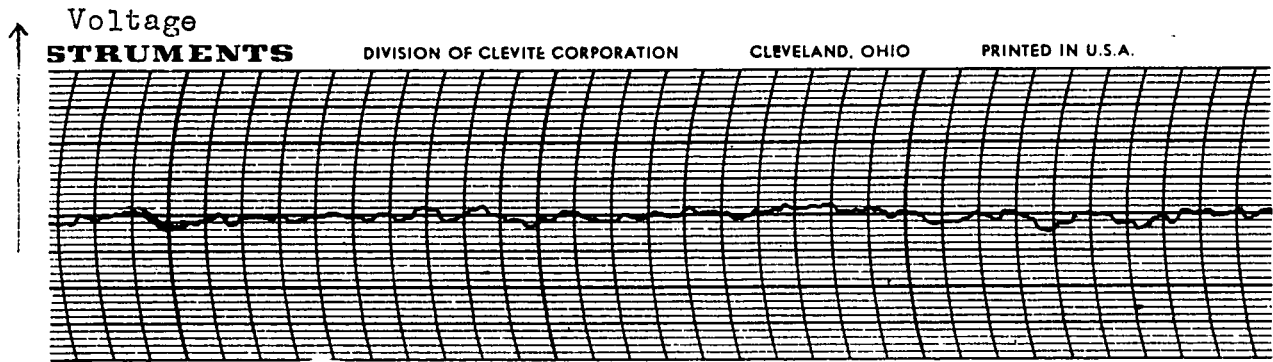
Hall output voltage V_H = $975 \mu v$

Hall Coefficient R_H = $95150 \text{ cm}^3/\text{coulomb}$

Sensitivity of the Hall element = 125.0 Volts/ampere-kilo gauss

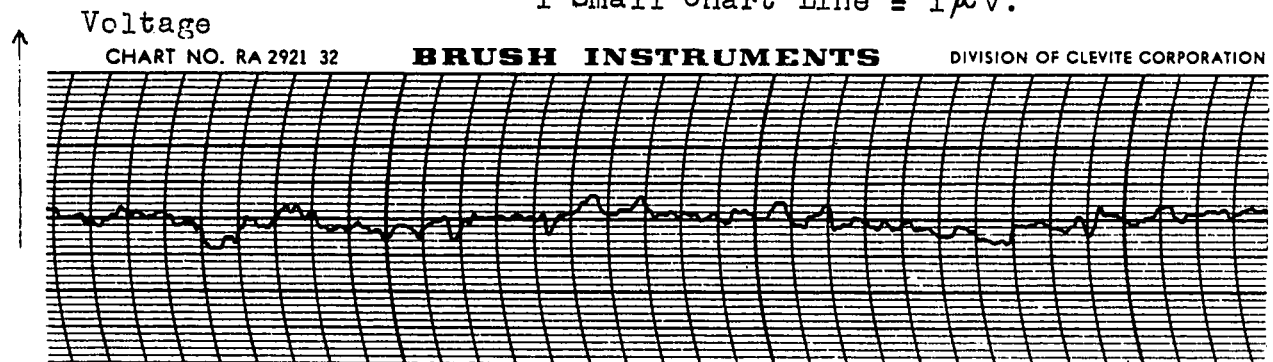
Zero field noise Voltage for
10 mA control current = $2.5 \mu v$ peak to peak (Fig. 4.9)

Zero field noise voltage for
15 mA control current = $5.5 \mu v$ peak to peak (Fig. 4.10)



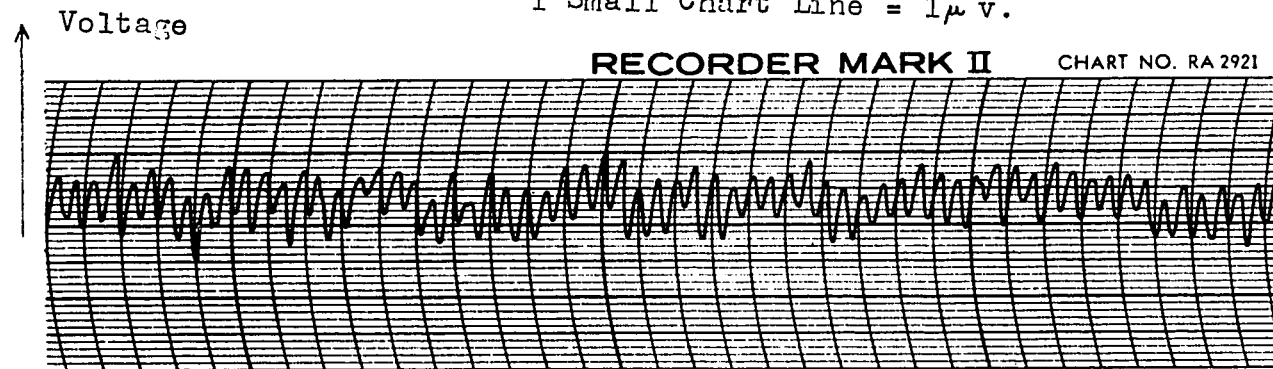
-----> Time

Fig. 4.9 Noise Voltage = 2.5μ v peak to peak.
Control Current = 10 mA.
Bandwidth = dc to 25 c/s.
1 Small Chart Line = 1μ v.



-----> Time

Fig. 4.10 Noise Voltage = 5.5μ v peak to peak.
Control Current = 15 mA.
Bandwidth = dc to 25 c/s.
1 Small Chart Line = 1μ v.



-----> Time

Fig. 4.11 Recording of 2×10^5 Gauss peak value
of frequency 10 c/s.
1 Chart Line = 1μ v.

2×10^{-5} Gauss peak value signal of 10 c/s frequency is recorded for 10 mA control current in the Hall element and is shown in the Fig. 4.11.

Fig. 4.12 shows the photograph of the same signal taken on memoscope. The scale on the scope was adjusted to $1 \mu\text{v}$ per cm.

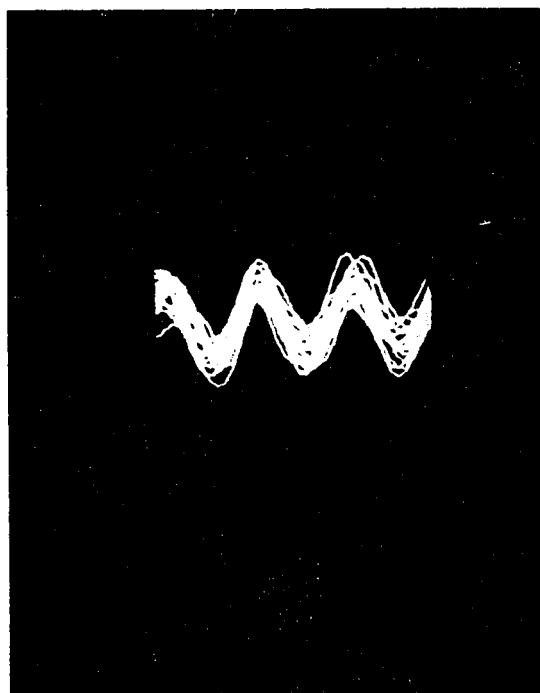


Fig. 4.12

Fig. 4.13 shows the Hall Co-efficient as a function of temperature.

SINGLE CRYSTAL AT LIQUID NITROGEN TEMPERATURE

Input resistance = 10.8 ohms

Control current = 50 mA

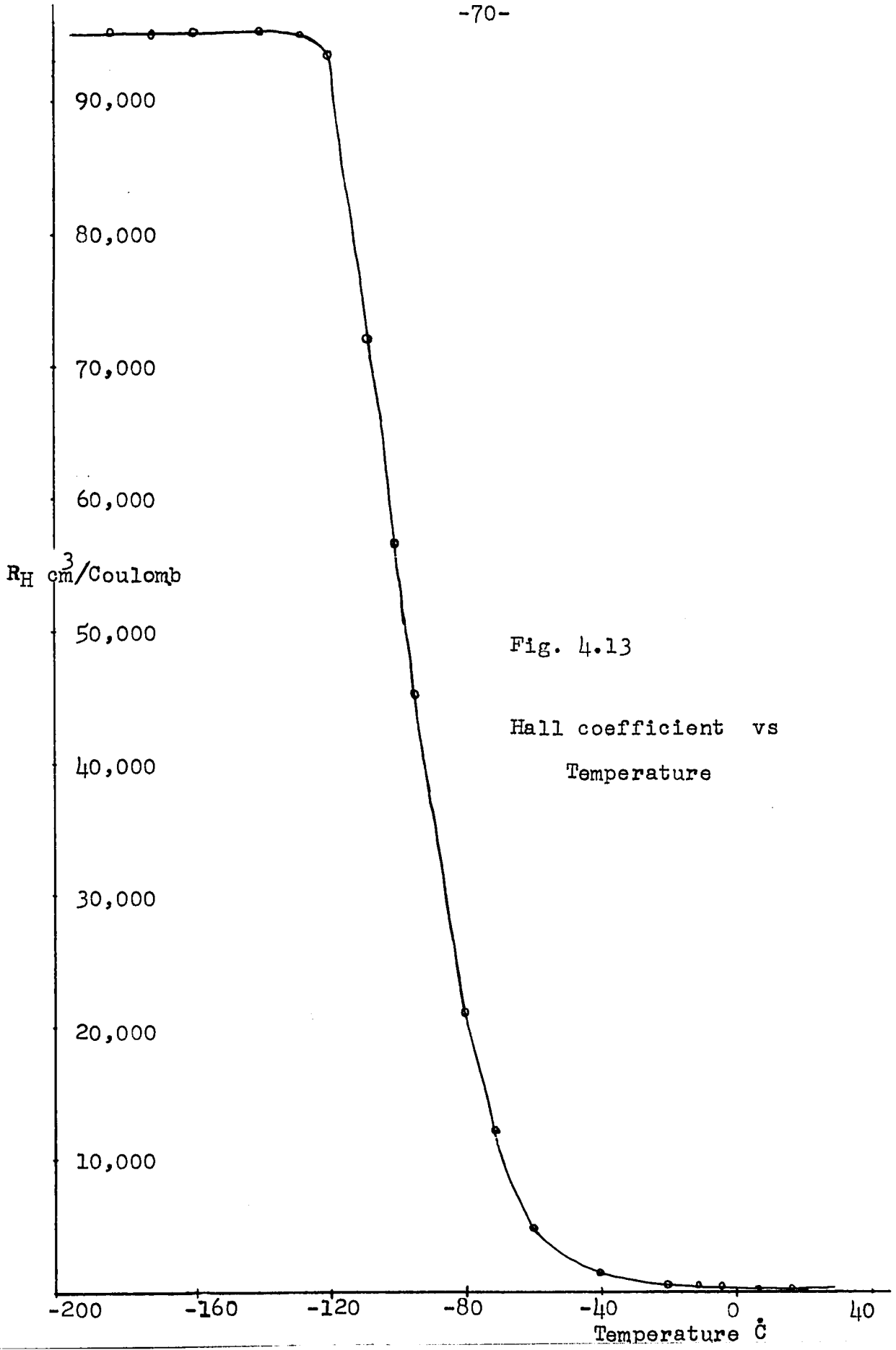


Fig. 4.13

Hall coefficient vs Temperature

Input power = 27 milliwatts
Magnetic field applied = 7.8×10^3 Gauss
Gain of the concentrator = 100
Hall output voltage V_H = $920 \mu v$
 $R_H = 17970 \text{ cm}^3/\text{coulomb}$
Sensitivity of the Hall element = 23.6 Volts /ampere-
kilo gauss

Zero field noise voltage
for 50 mA control current = $4 \mu v$ peak to peak (Fig. 4.14)
Zero field noise voltage
for 80 mA control current = $10 \mu v$ peak to peak (Fig. 4.15)

This device can detect a magnetic field of 3.4×10^5 Gauss peak value.

CONCLUSION

The overall sensitivity of the best Indium Antimonide Hall probe at liquid nitrogen temperature was 12500 volts per ampere-kilo gauss. The increase in sensitivity was due to high Hall coefficient, mobility and resistivity of the material. Even with this high sensitivity, the lowest measurable magnetic field should be of the order of 2×10^5 gauss peak (at a signal to noise ratio of unity.) Zero signal fluctuations in the output voltage remained approximately the same with and without the magnetic concentrator in the absence of the passing vehicles and moving permeable materials. This fact showed that the fluctuations in the output were produced inside the Hall element. The

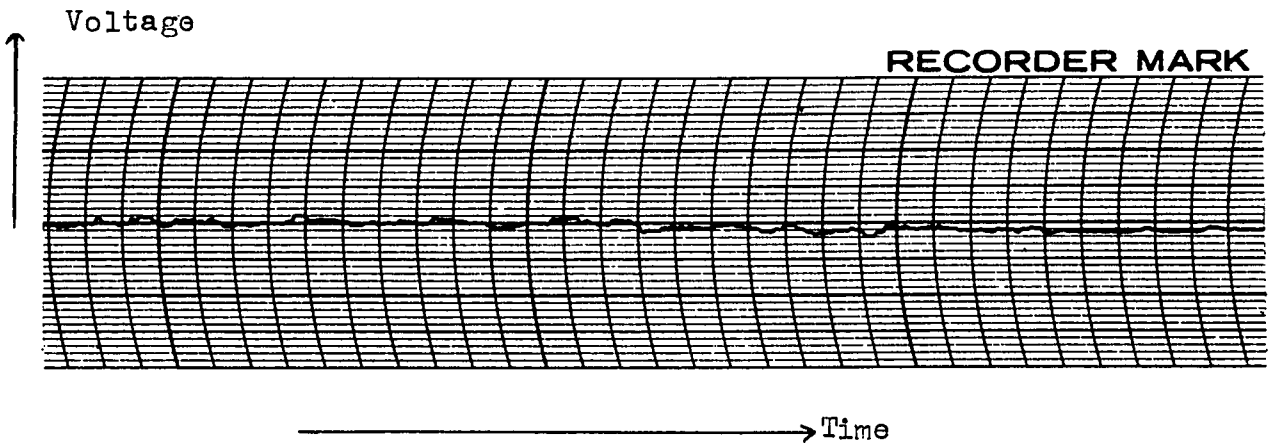


Fig. 4.14 Noise Voltage = $4\mu\text{v}$ peak to peak.
Control Current = 50 mA.
Bandwidth = dc to 25 c/s.
1 Small Chart Line = $2\mu\text{v}$.

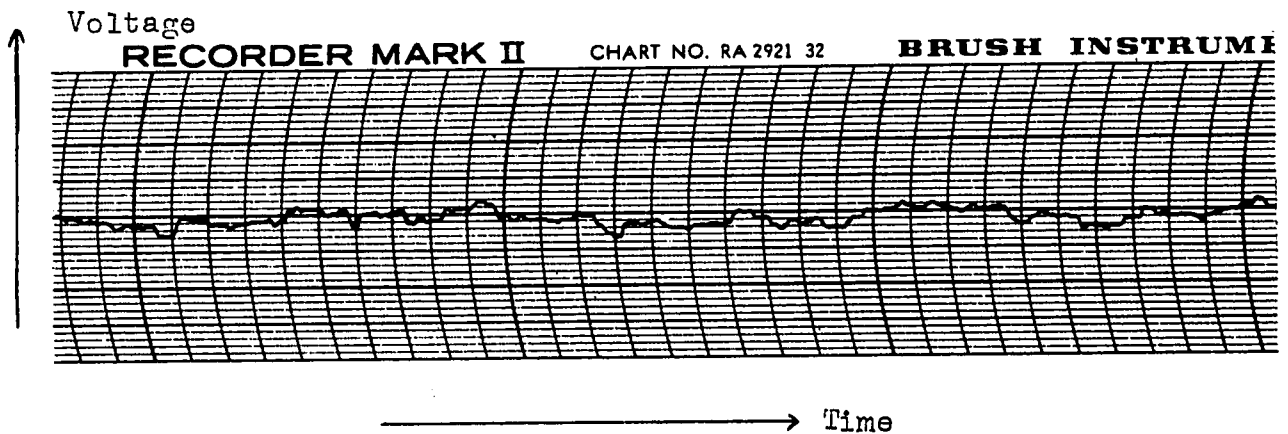


Fig. 4.15 Noise Voltage = $10\mu\text{v}$ peak to peak.
Control Current = 80 mA.
Bandwidth = dc to 25 c/s.
1 Small Chart Line = $2\mu\text{v}$.

cause of these fluctuations is attributed to (1) soldering of the contacts and (2) minute internal cracks and holes in the material.

The contacts could be improved by vacuum deposition of gold contacts. As regards to the internal cracks and holes, the material should be selected which is grown very slowly during the process of manufacturing. Low frequency unwanted fluctuations in the Hall output could be reduced considerably by passing ac control current of a few kilocycles frequency through the Hall element. The output of the Hall transducer, which is the product of the control current and the magnetic field, is then fed into an amplifier which is tuned to the frequency of the control current. The rectified output determines the strength of the unknown magnetic field.

This method will not eliminate the effects introduced in the output by the passing vehicles and the motion of the permeable materials. However, these effects can be reduced if the whole arrangement is built up in a well magnetically shielded room.

REFERENCES

1. Adams, G. D., Dressel, R. W., and Towsley, F. E. "A small milligaussmeter." Review of scientific instruments. Vol. 21 No. 1 Page 69, 1950.
2. McCurley, E. P. and Blake, C. "Simple null-indicating saturable core magnetometer for the detection of static magnetic fields" Review of scientific instrument. Vol. 31 No. 4 Page 440, April 1960.
3. "Magnetometer Model FM 1" Vickers Incorporated, Saint Louis 3, Missouri.
4. Wills, M. S. "A rotating coil fluxmeter" Journal of scientific Instruments. Vol. 29 Page 374, 1952.
5. Backstrom, G. "A device for the precision measurement of an inhomogeneous magnetic field" Nuclear Instrument 1 Page 253, 1957.
6. Semat, H. "Atomic and Nuclear Physics" Page 276, Chapman & Hall Ltd., London.
7. Vagola, G. K. and Bogalyrev, E. E. "High Precision Nuclear magnetic field strength meter" Measurement Techniques No. 9 April 1963.
8. Hurwitz, L. & Nelson, J. H. "Proton Vector Magnetometer" Journal of Geophysics, Vol. 65 No. 6 June 1960.
9. Pohen, A. V. and Rubens, S. N. "High sensitivity ballistic fluxmeter" Review of scientific instruments, Vol. 27 Page 306, 1956.

10. Lerond, P. and Thulin, A. "Sensitive recording magnetic fluxmeter" Journal of scientific instrument, Vol. 36 Page. 388, 1959.
11. Palmer, T. M. "Automotive compensation for thermal e-m-f's and galvanometer zero drift in a feedback fluxmeter" Journal of scientific instrument, Vol. 38 Page 209, 1961
12. Mazurov, M. E. "Induction method of measuring alternating magnetic fields" Measurement Techniques, Sept. 1962.
13. Birss, R. R. and Fry, J. P. "An electronic fluxmeter" Electronic engineering, Vol. 37 Page 31, 1960.
14. Gerhard Baule and McFee, R. "Detection of the magnetic field of the heart." American heart journal, Page 95 July 1963.
15. Bloom, A. L. "Principle of operation of the rubidium vapor magnetometer" Applied optics U.S.A. Vol. 1 No. 1 January 1962.
16. Dolan Mansir "Magnetic measurement of space" Electronics Vol. 33, August 1960.
17. McDermott, J. R. "Hall effect devices" Aerospace electronics, Vol. 35 No. 5 Page 146, 1961.
18. Barron Kemp "Hall-effect instrumentation" Howard, W. Sams & Co. Inc. Indianapolis 6, Indiana.
19. Milligan, N. P. & Burgess, J. P. "Hall effect devices for low level magnetic detection" Solid State Electronics Vol. 9 Page 323, 1964.

20. Kuhrt, V. F. "Eigenschaften der Hallgenetroen" Siemens-Zeitschrift Sept. 1954.
21. Roth, H. and Straub, W. D. "Very low offset Hall voltage" Journal of Applied Physics Vol. 33, Page 2397 1962.
22. Chasmar, R. P., Cohen, E. and Holmes, D. P. "The design and performance of Hall effect multiplier" A.E.I. Engineering Review, Vol. 1 No. 3 1960.
23. Glinski, G. S. and Landolt, J. P. "Theory and practice of Hall multiplier" Technical Report No. 61-3 Ottawa University 1961.
24. Lippman, H. J. and Kuhrt, F. "The influence of the geometry on the Hall effect in rectangular semiconductor plates" Z. Naturforschg 13a Page 474 1958.
25. Lindberg, Olof "Hall effect" Proceedings of the I.R.E. Vol. 40, Page 1414 1952.
26. Hilsum, C. "Galvanomagnetic effects and their applications" British Journal of Applied Physics Vol. 12, Page 85, 1961.
27. Saker, E. W., Cunnel, F. A., and Edmond, J. T. "Indium Antimonide as a fluxmeter material" British Journal of Applied Physics Vol. 6 Page 217, 1955.
28. Strutt, M. J. O. "Hall effect in semiconductor compounds" Electronic and Radio Engineer Page 2 January 1959.
29. Motto, J. W. "Using the Hall generator. A new control and instrumentation Component" Part II Automatic Control Page 24, July 1961.
30. Voeikov, D. D. "A method of increasing the equilibrium

- Stability of Hall probes" Soviet Physics Solid State
Page 2065 1958.
31. C. B. Burckhardt and M. J. D. Strutt "Noise in Non-reciprocal two ports based on Hall effect" I.E.E.E. Transaction on electron devices Feb. 1964.
 32. Sautter, D. "Noise in semiconductors" Progress in semiconductor Vol. 4 1960.
 33. Hrostowski, H. J., Morin, F. J., Geballe, T. H., and Wheatley, G. H. "Hall effect and conductivity of Indium Antimonide" Physical Review Vol. 100 No. 6
Page 1672 1955.
 34. Lofgren, L. "Analog Multiplier based on the Hall effect" Research Inst. of National Defence, Stockhom F.O.A. 3
Report 1957.
 35. Wood, C. "Hall effect transducer" Measurement Vol. 8
Page 138 1961.
 36. Ross, I. M., Saker, E. W., and Thompson, N.A.C. "The Hall effect compass" Journal of scientific instrument
Vol. 34 Page 479 1957.
 37. Kurt Warmth "Uber den ballististischen Entmagnetisierungsfaktor Zylindrischer Stabe" Archiv fur Elektrotechnik
Heft 5 1954.
 38. Parker, R. J. and Studders, R. J. "Permanent magnets and their applications" John Wiley and sons New York.

VITA

NAME: NAZIR AHMAD CHAUDHRY

BORN: India. April 11, 1935.

EDUCATION:

Matriculation: D. B. High School, 45 G. B.
Lyallpure, Pakistan.

Intermediate: Govt. College.
Quetta, Pakistan.

B.Sc. D. S. College.
Lahore, Pakistan.

M.Sc. Govt. College, Lahore.
Punjab University, Pakistan.

Course: Physics.

Degree: M.Sc., 1956.